Energy cost for force production is nonlinear and predicts human forces in legs, arms, fingers, and muscles

Sriram Sekaripuram Muralidhar[1,5,*,+], **Nadja Marin**[1,+], **Colin Melick**[1], **Hansol X Ryu**[1], **Aya Alwan**[1], **Zhengcan Wang**[1], **Ross Baldwin**[1], **Kristen Heitman**[6], **Sam Walcott**[4], **and Manoj Srinivasan**[1,2,3,*]

[1]Mechanical and Aerospace Engineering, The Ohio State University, Columbus OH 43201
[2]Program in Biophysics, The Ohio State University, Columbus OH 43201
[3]Ecology, Evolution, and Organismal Biology, Brown University, Providence RI 43201
[4]Mathematical Sciences, and Bioinformatics and Computational Biology, Worcester Polytechnic Institute, Worcester MA01609
[5]Biokinesiology and Physical Therapy, University of Southern California, Los Angeles CA 90007
[6]Health and Rehabilitation Sciences, The Ohio State University, Columbus OH 43201
[*]srirammu@usc.edu; srinivasan.88@osu.edu
[+]these authors contributed equally to this work

ABSTRACT

Muscles expend metabolic energy to produce force and movement, but how metabolic cost scales with force remains unresolved. Using human experiments involving sufficiently rich, time-varying forces with controls for force and force-rate confounds, we show that metabolic cost increases superlinearly with both force and force-rate, each well described by a power-law relation. Independent experiments involving nearly isometric knee extension confirmed the nonlinear dependence on force. To investigate physiological origins of this scaling, we developed mechanistic models of motor-unit recruitment, calcium handling, and force production, together with an analytical model of muscle pennation, showing that multiple physiological mechanisms naturally give rise to approximate power-law energetics. We further show that commonly used muscle metabolic models substantially underestimate measured metabolic costs. The nonlinear metabolic model accurately predicts how humans distribute forces between arms and between legs in two prospective experiments, whereas the widely used signal-dependent noise theory makes opposite predictions. The same framework explains previous observations of force sharing among fingers, predicts linear scaling of muscle forces and joint torques through a mathematical theorem, and remains valid in the presence of antagonist co-contraction. Finally, the model generalizes optimal feedback control by providing a physiologically grounded effort cost that predicts force fluctuation statistics. These results identify nonlinear metabolic cost as an important principle governing force production across muscles, limbs, and motor behaviors.

Introduction

Muscles consume metabolic energy to apply forces and produce movement. How such metabolic energy scales with muscle force critically determines how effortful each task is, and may shape how humans perform the task[1–8]. Thus, a central question is how metabolic energy use scales with muscle force and force changes, whether this scaling is linear[9–16] or nonlinear[17,18]. Resolving this question empirically is challenging because human-applied forces are never steady[19], and unsteady forces increase energy demands[20,21]. Prior *in vivo* experiments controlled only force or its rate of change, but not both, potentially conflating their respective energetic contributions[12,18,21,22]. Moreover, even if metabolic cost were shown to increase nonlinearly with force, its physiological origin would remain unclear, and it is unknown whether existing physiological models of muscle energetics can account for such measurements.

Here, we use diverse human metabolic experiments with appropriate controls for force and force-rate confounds (Figure 1A) to establish that metabolic cost increases superlinearly with both force and its rate of change, and independently confirm the nonlinear dependence on nearly isometric joint torques. We then investigate possible physiological origins of this scaling using mechanistic models of motor-unit recruitment, calcium handling, and force production, together with an analytical model of muscle pennation, showing that multiple physiological mechanisms naturally give rise to approximate power-law energetics. Finally, we compare our measurements with several widely used muscle metabolic models and show that they substantially underestimate experimentally measured metabolic costs.

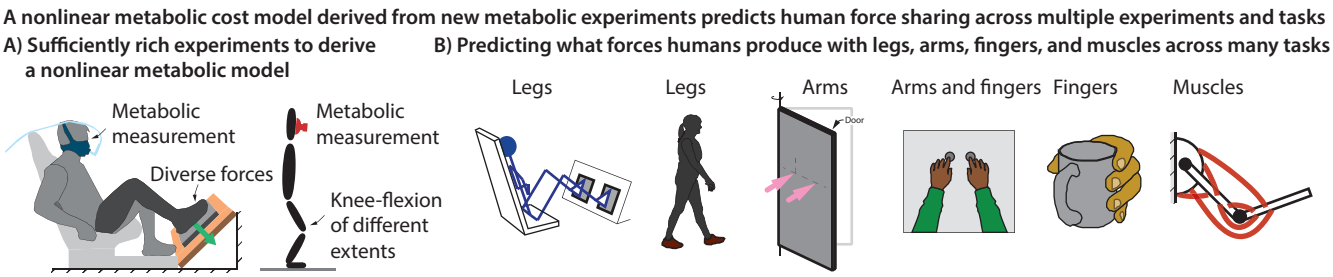

Figure 1. Nonlinear metabolic cost models and implications for human force choices. A) Through multiple behaviorally rich metabolic experiments, we derive a nonlinear model translating muscle forces, joint torques, and their rates of change into metabolic energy expenditure, unifying prior models into one framework. **B)** These models predict human force choices in two new experiments designed to distinguish competing theories and account for phenomena observed in past studies across legs, arms, fingers, and muscles.

If metabolic cost increases superlinearly with force, it should fundamentally influence how the nervous system distributes forces across muscles and limbs during motor tasks. Each motor task presents a human with infinitely many choices for what individual muscle forces to use and what forces to apply with different fingers, hands, arms, and legs. There are two competing theories of how the nervous system selects a unique solution from these infinitely many possibilities: humans may prefer motor patterns that minimize metabolic energy[1–8], or they may prefer patterns that minimize error or motor variability arising from signal-dependent noise[19,23,24]. Comparing these theories is challenging because they often produce correlated predictions[23]. We therefore perform two prospective experiments involving bilateral arm and leg forces designed to distinguish these theories, as well as to distinguish linear from nonlinear metabolic costs[25–29]. We show that the experimentally derived nonlinear metabolic model accurately predicts human force-sharing strategies, whereas predictions based on signal-dependent noise are anti-correlated with the observed behavior.

Beyond determining average force-sharing strategies, the experimentally derived nonlinear metabolic cost should also shape the moment-to-moment regulation of force and the variability that emerges during motor behavior. Optimal feedback control[24] is widely viewed as a general theory of sensorimotor control, predicting how humans balance task accuracy and effort during movement. However, previous formulations relied on ad hoc descriptions of effort[19,23,30,31]. Here, we generalize this framework using experimentally derived metabolic costs of force and force-rate to predict systematic changes in force fluctuations and temporal correlations during force production. We further show that the same power-law formulation explains force sharing across previous studies involving arms, legs, fingers, and muscles[23,32–34], prove that it predicts linear scaling of optimal muscle forces and joint torques across external loads, and demonstrate that this scaling is robust to antagonist co-contraction. Together, these results identify nonlinear metabolic cost as a unifying principle connecting muscle physiology, biomechanics, and sensorimotor control across multiple levels of organization.

Results

Experiment: Metabolic cost for time-varying forces is described by power-law force and force-rate costs. We measured the metabolic energy expenditure of human participants applying periodic leg forces (Figure 2A) of substantial diversity with varying means, amplitudes, time periods, rise times and fall times (Figure 2B), yielding 297 trials across 11 participants and over 30 hours of data. Participants tracked forces precisely enough to disambiguate dependencies on force and force changes (Supplementary Figure S1). From this data, we obtain a power-law model (equation 1) incorporating force, positive force-rate, and negative force-rate terms:

$$\dot{E}_{\text{model}} = a_0 + a_1 F_{\text{ext}}^{\gamma_1} + a_2 (\dot{F}_{\text{ext}})_{\text{pos}}^{\gamma_2} + a_3 (\dot{F}_{\text{ext}})_{\text{neg}}^{\gamma_2}. \tag{1}$$

The force exponent was about $\gamma_1 = 1.4$ and the force-rate exponent was $\gamma_2 = 2.6$ (Figure 3C), with $R^2 = 79.4\%$ (Figure 3D), indicating the model captures the data well. Both exponents exceed 1, showing that metabolic cost scales superlinearly with force and force rate (Figure 3A,B).

Theory: A mechanistic muscle model predicts superlinear metabolic costs. To investigate potential physiological origins of the observed power-law relation, we developed a muscle model combining motor-unit recruitment, calcium handling, SERCA pumping, and force production (Supplementary Section S1.1 and Supplementary Figure S6). Although actomyosin energetic cost was assumed linear in force, the combined effects of recruitment, calcium cycling, and activation dynamics produced an overall metabolic cost that increased approximately as a power law with force, consistent with our experimental exponent.

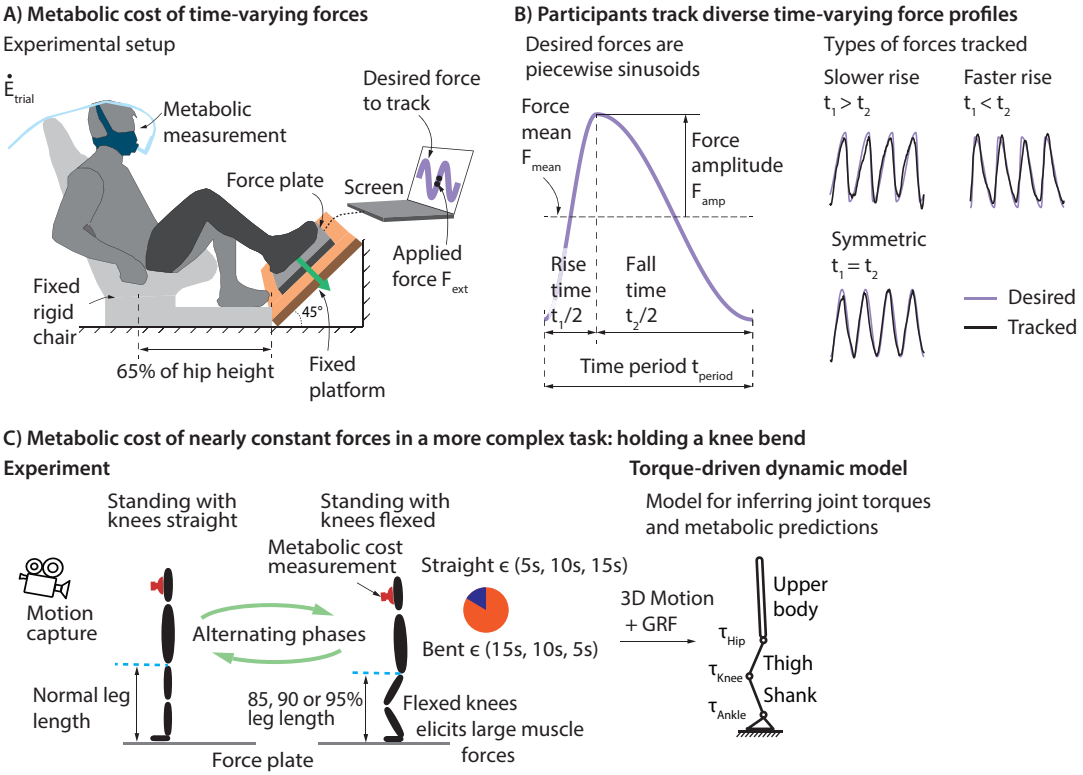

Figure 2. Two metabolic experiments for isolating the cost of force and force changes. A) While seated in a rigid chair, humans apply leg forces on a platform, tracking various desired force profiles shown on a screen. Each desired force is a piecewise sinusoid combining two sinusoids with the same mean (F_{mean}) and amplitude (F_{amp}), but possibly different rise ($t_1/2$) and fall ($t_2/2$) periods. We varied means, amplitudes, and time periods across trials, yielding a diverse dataset. **B)** Participants alternated between quiet standing and knee-flexed standing with visual feedback, for different knee-flex leg lengths and duty factors. We estimated metabolic cost from respiratory gases, limb motion with optical motion capture, ground reaction forces with force plates, and joint torques via inverse dynamics. We derive a power-law metabolic cost model for force and force-rates from these experiments.

Ablation studies showed that multiple physiological mechanisms contribute to this emergent nonlinearity, indicating that the observed scaling does not depend on any single modeling assumption. Power-law fits to the model-predicted metabolic costs also result in an exponent of about 1.5, close to that obtained from experiments.

Theory: Pennation further increases the nonlinearity of force production costs. We next asked whether muscle architecture alone could contribute to nonlinear metabolic costs. A simple analytical model showed that, because pennation angle increases with force as tendons stretch, tendon force becomes a nonlinear function of muscle-fiber force even when individual fiber metabolic cost is exactly linear (Supplementary Section S1.2), with weak nonlinearity in slightly pennate muscles and stronger nonlinearity in highly pennate muscles.

Experiment: Non-zero force-rates increase metabolic costs. Given the positive force-rate exponent ($\gamma_2 \approx 2.6$), increased force-rates, even when controlling for force, led to higher metabolic expenditures[21]. Omitting the force-rate term yielded a poorer fit (Figure 3E). Specifically, using a train-test cross-validation with 80% of data for training and 20% for testing, we found that including the force-rate term reduced both the training error ($p = 10^{-39}$, one-sided t-test) and the test error ($p = 0.004$, one-sided t-test) by about 5% compared to the baseline model (Figure 3E).

Experiment: Decreasing forces quickly cost more than increasing force. Our model allowed different costs for positive and negative force rates. The coefficient for negative force rate was about three times that for positive force rate ($a_3 = 0.0155$, p-value = 10^{-6}; $a_2 = 0.0049$, p-value = 0.045, Figure 3B). To confirm this difference was not due to random variability, we repeated the regression after randomly shuffling positive and negative force-rate values. Shuffling produced $a_3 - a_2$ values near 10^{-8}, whereas the correct unshuffled data yielded $a_3 - a_2 = 0.0105$, significant at $p = 10^{-51}$ (one-sided t-test, Figure 3F).

Experiment: Independent experiment confirms nonlinear metabolic dependence on force. We verified the nonlinear metabolic cost of joint torque through an independent experiment (Figure 2B). Participants alternated between quiet standing and knee-flexed standing, during which muscles were nearly isometric (Figure 3G, see *Methods*). Principal component analysis of joint torques estimated via inverse dynamics showed the first component explained over 90% of torque variance (Figure 3H), allowing omission of joint-specific cost coefficients. Fitting a power-law model yielded an exponent $\gamma_1 = 1.64$, close to the earlier $\gamma_1 = 1.4$, with similar predictive power (Figure 3I). Thus, metabolic cost of isometric torque scales superlinearly, with exponent $\gamma_1 > 1$.

Model: Prior metabolic models underestimate measured metabolic costs. We compared experimentally measured metabolic expenditure with predictions from several widely used muscle metabolic models, including the Umberger, Bhargava, and Alexander–Minetti formulations, as well as mechanical work estimated from tendon deformation (Supplementary Section S2.1 and Supplementary Figure S4). Although these models captured some qualitative features, they consistently underestimated the magnitude of measured metabolic cost, explaining only a modest fraction of the observed energy expenditure. These comparisons suggest that a superlinear dependence on force provides a substantially more accurate description of metabolic cost in the present tasks.

Theory: Optimization with the power-law metabolic model explains force sharing between arms and between legs. Metabolic effort may influence how humans perform sensorimotor tasks, so we demonstrate the implications of the nonlinear metabolic model by predicting human-generated forces in motor tasks. We performed two prospective experiments in which participants produced goal forces using both hands or both legs, admitting infinitely many ways to achieve a fixed goal force (F_{goal}) expressed as $F_{\text{output}} = \lambda F_{\text{left}} + (1-\lambda)F_{\text{right}}$ (Figure 4A,B). This task is analogous to applying a moment with two limbs, such as pushing a door with both hands (Figure 4C). The coefficients λ and $(1-\lambda)$ represent the output's sensitivity to the left and right forces; $\lambda = 1$ and $\lambda = 0$ correspond to sensitivity only to the left or right force, respectively. We tested two goal force levels, $\alpha = 0.40$ and 0.70, measured as fractions of maximum comfortable force (*Materials and Methods*). Participants tracked these goal forces accurately on average (Figure 3D).

We use the power-law metabolic model to approximate the energy cost of this task as $\dot{E}_{\text{met}} = (F_{\text{left}} - \beta_{\text{left}})^{\gamma_1} + (F_{\text{right}} - \beta_{\text{right}})^{\gamma_1}$, where β represents passive external forces when the limbs rest passively on the force plates. Constrained minimization of this metabolic cost predicts force sharing (Figure 4D), yielding distinct outcomes for different exponents γ_1 (Figure 4E). For $\beta = 0$, a nonlinear exponent ($\gamma_1 = 2$) yields linear sharing with λ, while a near-linear cost ($\gamma_1 \approx 1$) flattens the energy landscape, predicting "all-or-nothing" force-sharing, with one limb contributing fully depending on λ.

Metabolic model predictions with exponent $\gamma_1 = 1.4$ matched the human force trends closely in both lower-limb and upper-limb experiments. In lower-limb experiments, both goal force levels showed greater force on the limb contributing more to the output, with asymmetry depending on λ and force level (Figure 3G). Upper-limb experiments showed similar trends, though less pronounced at lower goal forces (Figure 3H). The model reproduced these sigmoidal force-sharing dependencies ($R^2 = 73.8\%$ upper limb, $R^2 = 79.6\%$ lower limb), and predicted symmetric force sharing for $\lambda = 0.5$, consistent with data. Using the empirically derived metabolic exponent ($\gamma_1 \approx 1.4$) outperformed the quadratic exponent ($\gamma_1 = 2$) commonly assumed in the literature without any metabolic basis (Supplementary Figure S2).

Alternative theory: Minimizing signal-dependent noise-based variability does not predict arm and leg forces. An influential alternative to metabolic cost minimization is minimizing motor variability from signal-dependent and sensory noise[19,23] and sensory noise. Our experiment was designed to distinguish these theories, as they predict opposite outcomes. We vary the contribution λ independently of muscle properties unlike some prior work[23], whose equivalent λ were constrained by muscle properties. To make predictions, we modeled output force error variance, arising from signal-dependent noise, as the minimized cost, assuming zero mean error (*Methods*). For $\lambda \approx 1$, this theory predicts higher right-side force, and for $\lambda \approx 0$, lower right-side force. These predictions are opposite to observed human behavior (Figure 5A-B) and to metabolic model predictions (Figure 4G,H), yielding negative R^2 values. Hybrid models combining variability and metabolic costs into a weighted sum (δ metabolic cost + $(1-\delta)$ variability) offered no improvement; the best-fit weighting $\delta \approx 1$ indicated variability minimization played a negligible role in predicting force sharing.

Theorem: Metabolic power-law scaling predicts linear muscle force scaling. Thus far, we have framed the power law metabolic cost model as being a function of joint torques or of external force. Now, we generalize the power-law metabolic model to muscle forces and show its self-consistency across scale: muscles, joints, and limbs. To show this self-consistency, we first show that minimizing the power-law metabolic cost yields a linear scaling of muscle forces, consistent with experiments, as seen in experiments[32,33].

Consider producing external forces of varying magnitudes but fixed direction using a multi-joint limb at rest (Figure 6E). Minimizing power-law metabolic cost produces a "linear scaling strategy": once the optimal muscle forces are found for one force magnitude, solutions for any other are simple scalar multiples[32]. In more detail, consider a task in which a multi-joint

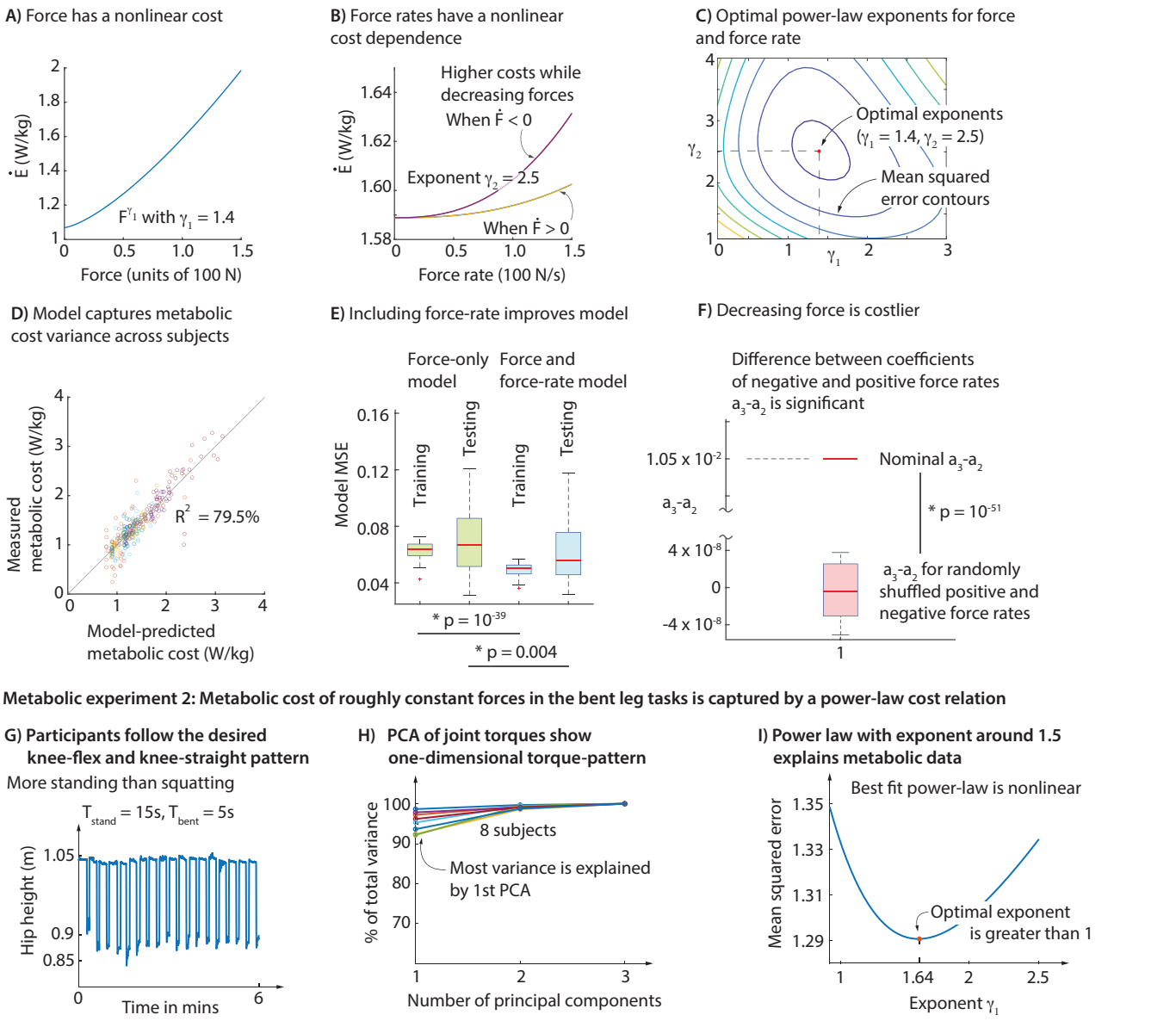

Figure 3. Power law model for the metabolic cost of force and force-rates. A) Best-fit force-dependence of metabolic cost is nonlinear — specifically, superlinear — fit by the power-law exponent $\gamma_1 = 1.40$. The curve shows model metabolic cost when the force is constant and force rate is zero. **B)** Best-fit force-rate-dependent of metabolic cost has a strong nonlinearity (exponent $\gamma_2 = 2.5$). Curves show model metabolic cost terms for positive and negative force-rate when the nominal force equals 100 N in our experiment. **C)** Mean squared error of model versus experimental data is minimized at $\gamma_1 = 1.40$ and $\gamma_2 = 2.5$. **D)** The best-fit model predicts the data well, with a high R^2 value of 79.5% across all participants. **E)** Mean squared error is lower for the model having both force and force rate terms, as opposed to having only force term. **F)** The coefficients for positive and negative force rates are significantly different. Repeated regression using randomly shuffled positive and negative force rate values gives $a_3 - a_2$ of about 10^{-8}, which is different from the nominal value, suggesting statistical significance of this difference. **G)** Hip marker height data for a participant during 3 different trials, showing the up-down movement of the hip, corresponding to straightening and bending the knee. **H)** Principal component analysis of ankle, knee, and hip joint torques across all trials shows that the first component explains most of the torque variance. **I)** Mean squared error between model prediction and experimentally measured energy rate across all participants and trials is minimized at $\gamma_1 = 1.64$, but with a flat error landscape such that $\gamma_1 = 1.4$ has similar error.

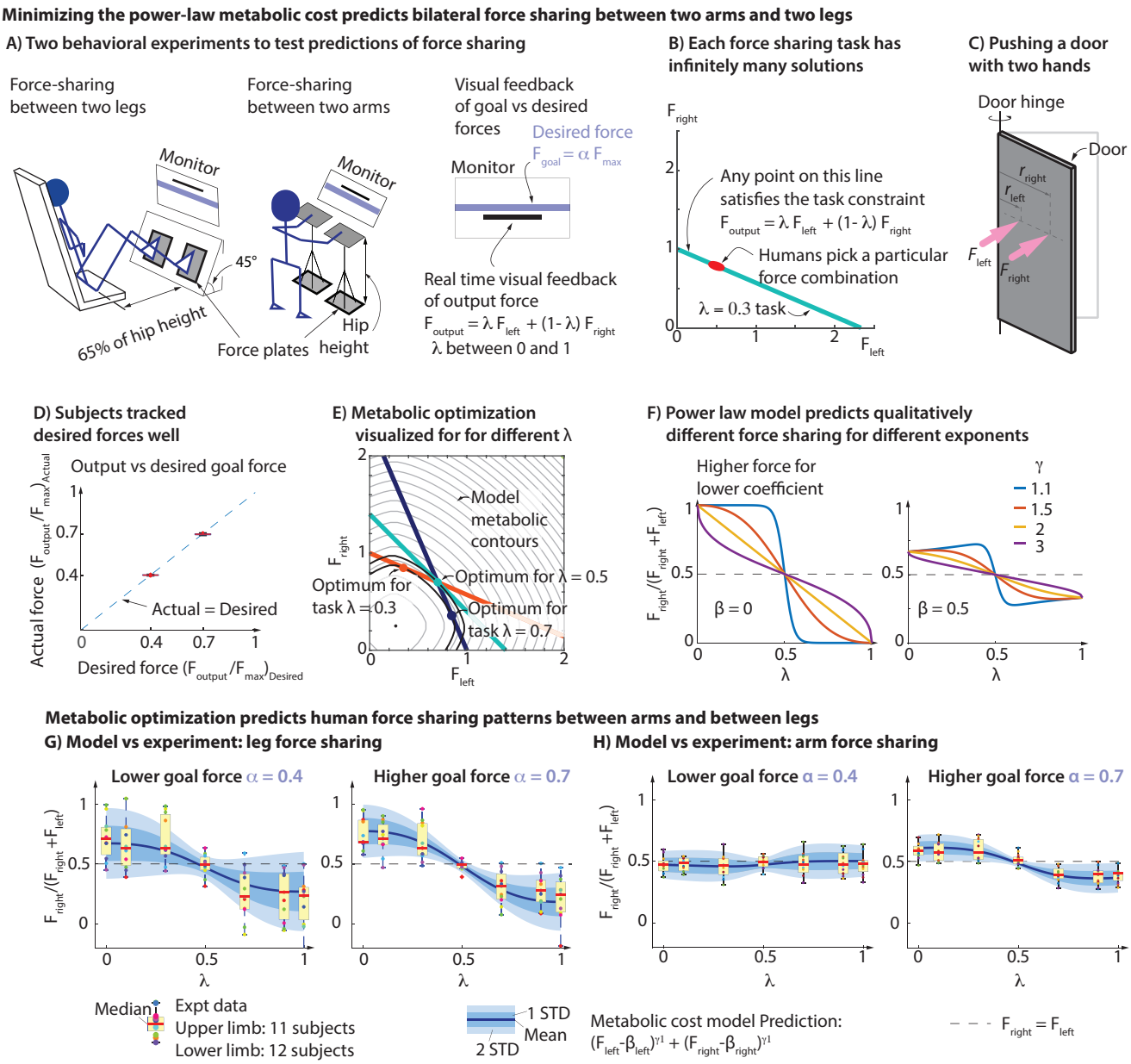

Figure 4. Nonlinear metabolic model predicts human force sharing between arms and between legs. A) Participants apply forces with arms or legs to maintain a fixed goal force (violet rectangle) using visual feedback. For arms, they stand and press down vertically on the platforms; for legs, they sit with arms crossed and press on the force plates. The participant's output force is a weighted sum of normal forces on each force plate, shown in real time (black line). **B)** The force-sharing task admits infinitely many solutions, namely, the cyan line segment $\lambda F_{\text{left}} + (1-\lambda) F_{\text{right}}$. Humans generally converge to a small region on this line segment, revealing their force-sharing strategy. **C)** This task is mathematically equivalent to pushing a door with two hands. **D)** In the experiments, participants' force output averaged across second half of the trials accurately tracks the desired force output. Box plot pools all trials and all participants in both upper and lower limb experiments. **E)** Metabolic optimization visualized geometrically: at the optimum, task constraints (violet, cyan, red) for $\lambda = 0.7, 0.5, 0.3$ are tangent to metabolic cost contours (gray). The center of the cost contours is when limbs rest passively, applying force $(\beta_{\text{left}}, \beta_{\text{right}})$. **F)** Different exponents γ_1 predict qualitatively distinct force-sharing patterns with varying λ and β. **G–H)** Model predictions agree with experimental data for legs and arms across force contributions (λ) and goal force levels ($\alpha = 0.4, 0.7$).

(open-chain) limb with m muscles (Figure 6E) is at rest and needs to apply a 3D external force $\mathbf{F}_{\text{ext}} = \mu \mathbf{F}_0$, a scaled version of

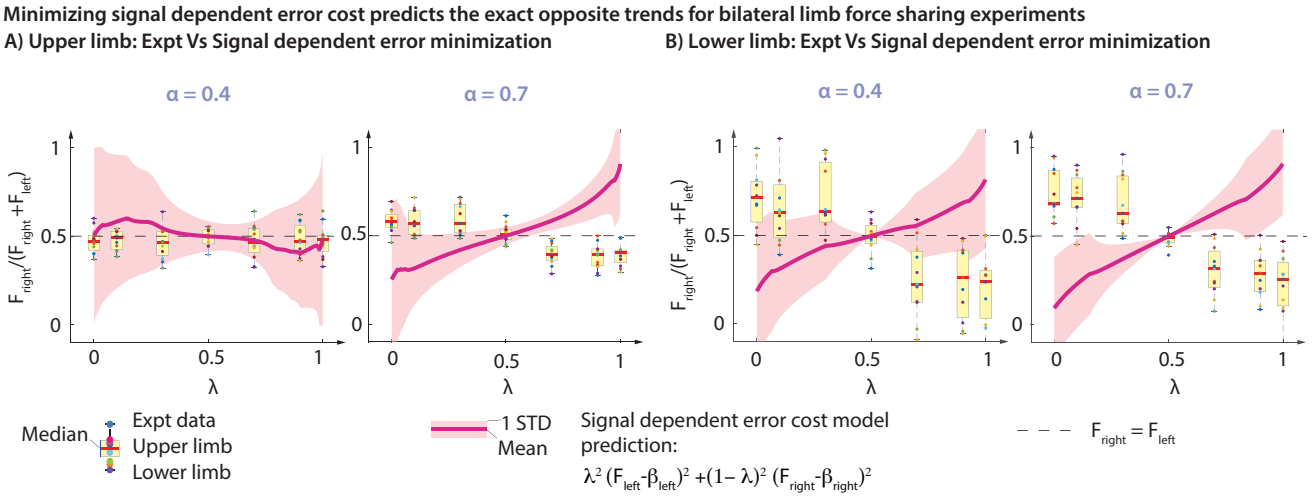

Figure 5. Signal dependent error cost does not predict force sharing. A) Upper limb model predictions versus experimental data. **B)** Lower limb model predictions versus data. The signal-dependent error cost fails to predict observed force sharing and instead produces behavior qualitatively opposite to human choices.

some nominal force $\mathbf{F}_0$, where μ is a positive scalar. We minimize a muscle-level power-law metabolic cost: $\dot{E} = C^T \mathbf{F}_{\text{mus}}^{\gamma_1}$, a weighted sum of the muscle forces raised to the same exponent γ_1. Then, if the energy optimal muscle force magnitudes for the nominal external force $\mathbf{F}_0$ are $\mathbf{F}_{\text{mus0}} \in \mathbb{R}^m$, the optimal muscle force magnitudes for any other external force $\mu\mathbf{F}_0$ are given by $\mu\mathbf{F}_{\text{mus0}}$, assuming external forces dominate gravity. The Supplementary Appendix provides a proof, corollaries, and generalization to time-varying forces including both force and force-rate costs.

Corollary 1: Whole-limb cost scales like muscle-level cost. If individual muscle metabolic costs scale with force to the power γ_1, the total limb cost scales similarly, as μ^{γ_1}:

$$\text{Metabolic cost } = C^T \mathbf{F}_{\text{mus}}^{\gamma} = \mu^{\gamma} (C^T \mathbf{F}_{\text{mus0}}^{\gamma}). \tag{2}$$

Here, $(C^T \mathbf{F}_{\text{mus0}}^{\gamma})$ is constant. Since external force magnitude $|\mathbf{F}_{\text{ext}}| = \mu |\mathbf{F}_0|$ is proportional to μ, the metabolic cost scales like external force magnitude raised to the power γ. This corollary demonstrates the self-consistency of the power-law metabolic model from muscle to limb scale, supporting the generality of the external-force-based model (equation 1).

Corollary 2: Optimality of linear muscle force and torque scaling strategy. At a given configuration, joint torques are linear in muscle forces:

$$\tau = D\mathbf{F}_{\text{mus}} = \mu\, D\mathbf{F}_{\text{mus0}}, \tag{3}$$

where D is a matrix of muscle moment arms. Each joint torque is thus proportional to μ and scales linearly with the external force magnitude $|\mathbf{F}_{\text{ext}}|$. Consequently, when scaling the external force in a fixed limb configuration, the metabolic cost scales with joint torque magnitude raised to the power γ_1.

Model predictions: Linear muscle-force scaling is robust to antagonist co-contraction. Our theoretical prediction that optimal muscle forces scale linearly with external force assumes identical power-law exponents across muscles. We tested whether this property is altered by antagonist co-contraction using a muscle-driven leg model with experimentally motivated coactivation constraints (Supplementary Sections S2.2 and Supplementary Figure S5). Although co-contraction increased overall muscle activation, the optimal solution remained a linear scaling of muscle forces with external force. Thus, the predicted power-law scaling of whole-limb metabolic cost is robust to moderate antagonist co-contraction.

Model predictions: Metabolic model with finger-specific coefficients predicts bimanual finger force sharing. Morrison and Newell[33] studied bilateral finger force sharing where participants produced a fixed total finger force (Figure 6A). Forces increased linearly with total force, consistent with our model (Figure 6B, $R^2 = 99.9$, $p < 10^{-5}$). This required different coefficients for each hand, with the stronger right hand having a smaller coefficient (1.02 left, 0.88 right).

O'Sullivan et al.[23] reported distinct sharing patterns across four finger pairs: left index-right index, left little-right index, left index-right little, left little-right little (Figure 6A). To explain their results, they had to use a force-dependent weighting of

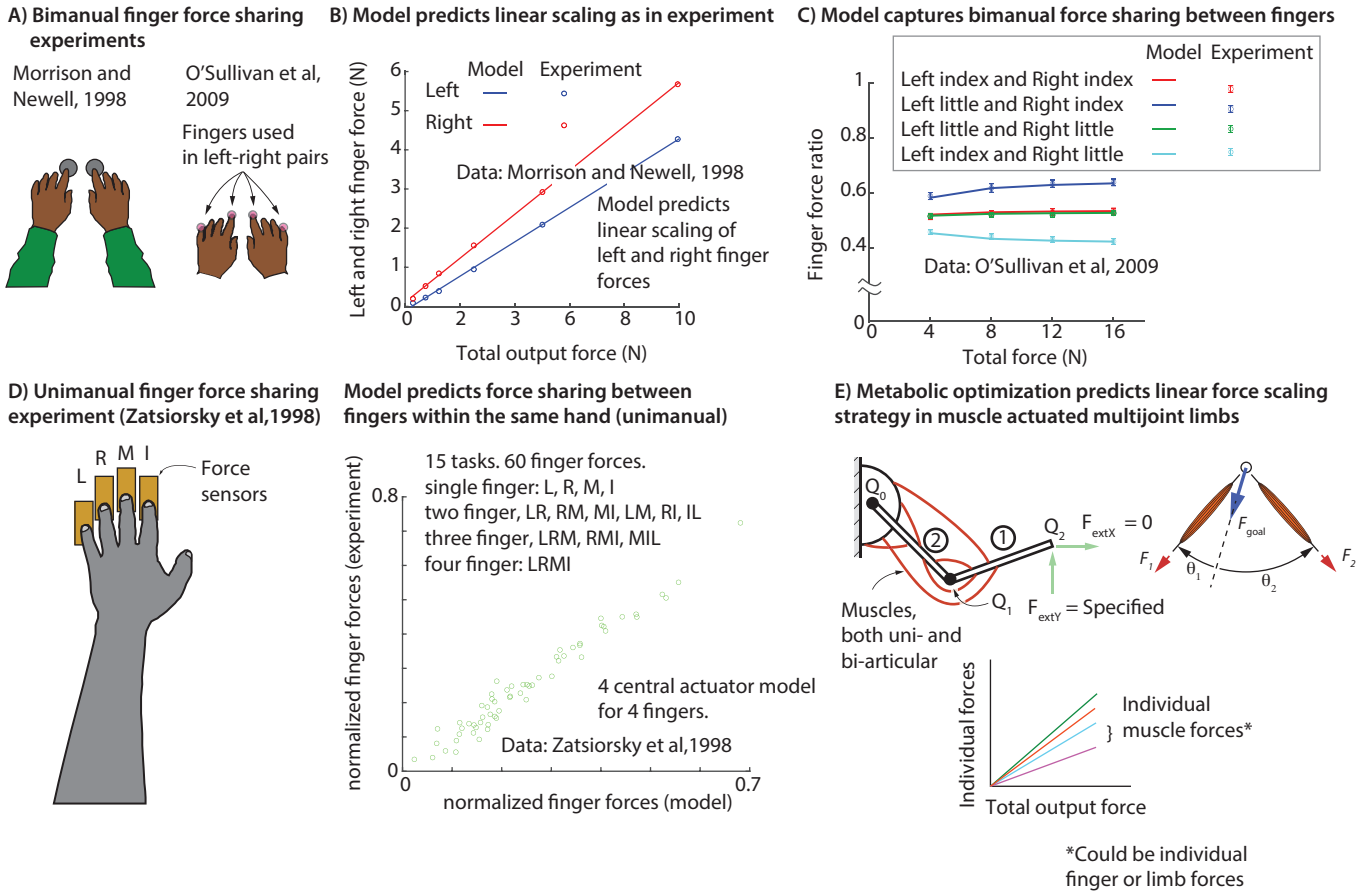

Figure 6. Metabolic model captures bimanual finger force sharing. A) Two different studies[23,33] asked participants to apply forces using fingers on the two hands, so as to attain total target forces of different magnitudes: one study involved the index fingers from each hand[33] and the other study considered all possible two-finger combinations of little and index fingers on left and right hands[23]. **B)** When producing forces with both index fingers, participants produced different total forces by a linear scaling strategy[33]; the linear strategy predicted by metabolic optimization captures the forces produced by the participants with 99.8% R^2 for both left and right fingers. **C)** Metabolic optimization with a single set of force-independent cost coefficients explain the relative force sharing between index and little fingers of the left and right hand[23]. This model predicts the forces much better than a composite cost consisting of an effort cost that scales with maximum force and signal dependent variability[23]. **Model captures unimanual finger force sharing. D** Participants were asked to produce forces with one or more specific fingers from the four contacting fingers[34]. Producing force with one or more fingers results in 'parasitic' forces from other uninvolved fingers. **E)** Minimizing power law metabolic cost function captures the individual finger forces in the involved and uninvolved fingers, without the use of any task-specific parameters. A sufficient model involves force production with four muscles, each of which can affect multiple fingers. **F) Force sharing between muscles.** When there are multiple muscles and multiple joints that contribute to an external force, minimizing the power law metabolic model predicts linear scaling of individual muscle forces with external force, as seen in experiments[32].

effort and signal dependent noise costs. In contrast, we explain all four conditions with a single finger-specific parameter set, independent of the external force produced (Figure 6C).

Model predictions: Metabolic model explains finger forces within a hand. Force sharing between fingers in the same hand is potentially more complex due to coupled actuation of fingers. When several fingers contact a surface, attempting to produce force with selected fingers also generates unintended "parasitic forces" in others. Zatsiorsky et al[34] studied this by asking participants to produce force with specific combinations of the four non-thumb fingers (index, middle, ring, little), yielding 15 combinations (Figure 6D). They measured all finger forces, including parasitic ones. While their neural-network model required task-specific parameters, we show that the same data are explained by a task-independent metabolic objective with

constant coefficients (Figure 6D); a model with four muscles coupled in actuating the finger forces was sufficient.

Model predictions: Force fluctuation statistics during force-sharing are explained by metabolic cost minimization via optimal feedback control. In force-sharing tasks, individual limb force fluctuations are correlated rather than independent, with correlations varying systematically with λ: forces are most negatively correlated at $\lambda = 0.5$ and nearly uncorrelated near $\lambda = 0$ or 1 (Figure 7A-B; see also[28]). This pattern is consistent with the concept of an "uncontrolled manifold," where variability orthogonal to the task manifold—contributing to task error—is more strongly corrected than variability along it. Todorov and Jordan[24] proposed that such correlations arise from optimal feedback control, balancing task error from signal-dependent noise with effort. But, they did not compare such predicted force correlations with a targeted experiment and their effort cost was a non-metabolic quadratic cost. Here, we derive an optimal feedback controller minimizing task error with effort cost defined by our power-law metabolic model, which qualitatively predicts both the observed correlations and their systematic change with λ (Figure 7C). The new force-rate cost is critical for these results, as a purely force-cost is not sufficient for the optimal control problem to produce these results. Further, incorporating the force-rate costs in the objective makes the predicted average forces slightly more symmetric than a purely force cost, even under asymmetric

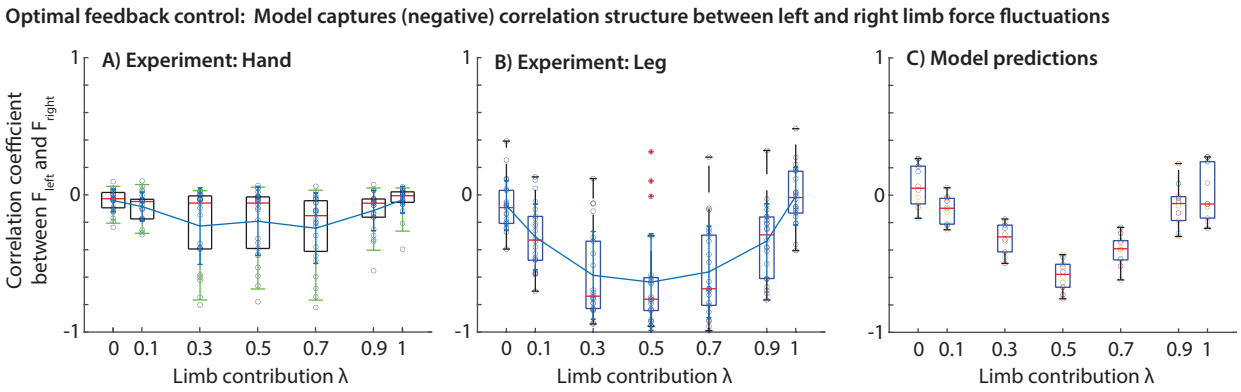

Figure 7. Model captures force correlations and control. In the **A)** arm force sharing experiments and **B)** the leg force sharing experiments (Figure 4A), the individual hand or leg forces F_{left} and F_{right} showed systematically different correlations within a trial depending on the λ value. The limb forces were least correlated for λ equalling 0 or 1, and negatively correlated for $\lambda = 0.5$. **C)** Minimizing the metabolic cost model while trading off against a task error term using an optimal feedback control framework predicts such systematic correlations. This optimization critically requires the nonlinear force rate cost in addition to the force cost.

Discussion

We derived a metabolic cost model for time-varying isometric muscle contractions showing superlinear power-law scaling: cost increased with joint torque or external force with exponent $\gamma_1 \approx 1.4$, and with torque or force rate with exponent $\gamma_2 \approx 2.5$. Earlier studies investigating force-dependent energetics generally did not independently control force and force-rate fluctuations as we did[18,35,36], making it difficult to separate their energetic contributions. Our results contrast with earlier reports of linear force dependence, which were largely based on isolated muscle preparations[9–11] or *in vivo* measurements at relatively low force levels[12,13]. Although the physiological origins of this power law remain to be established experimentally, our simple mechanistic models demonstrate that nonlinear force energetics emerge naturally from multiple physiological features, including motor-unit recruitment, calcium handling, and muscle pennation. Importantly, the approximate power-law relation proved robust across a wide range of model assumptions, parameters, and ablation analyses, suggesting that it may reflect a general consequence of muscle physiology rather than any single mechanism.

The experimentally derived power-law metabolic model accurately predicted force sharing between arms and legs in two prospective experiments, as well as force sharing reported previously across bilateral finger pairs, within-hand fingers, and individual muscles. Although the metabolic experiments were performed only on lower limbs, the same model explained behavior across multiple effectors and scales, suggesting that a common energetic principle may govern force production throughout the neuromuscular system. We further showed theoretically that if individual muscles obey the same power-law energetics, optimal muscle forces, joint torques, and external forces all exhibit the same scaling relation. This self-similarity remained valid even when antagonist co-contraction was incorporated into the optimization, indicating that the predicted scaling is robust to moderate deviations from idealized muscle recruitment.

Using the commonly assumed quadratic effort model ($\gamma_1 = 2$)[23,37] resulted in poorer fits to both metabolic data and force-sharing behavior than the experimentally derived exponent, consistent with earlier observations that quadratic objectives often require additional linear terms[38]. Likewise, a cost based on signal-dependent noise predicted force-sharing patterns opposite to those observed experimentally, and combining it with metabolic cost did not improve predictions. We also found that several widely used physiological metabolic models, including those of Umberger, Bhargava, and Alexander–Minetti, substantially underestimated measured metabolic costs in our experiments. Although these models were developed for broader movement conditions than the present isometric tasks, the comparisons suggest that incorporating the experimentally observed superlinear dependence on force may improve future metabolic models.

In our study, the contractions were only approximately isometric because of tendon compliance, and our analysis neglected possible effects of muscle length, contraction velocity, and joint configuration, although we independently examined deviations from isometry with a leg model to show that this may be a small effect. Because joint torques remained highly correlated during the standing experiments, we could not estimate joint-specific energetic coefficients independently. Likewise, the mechanistic muscle models were intentionally simplified and were intended to test plausibility rather than provide detailed physiological descriptions. Future work should combine richer experimental paradigms with muscle imaging, electromyography, tendon mechanics, and multiscale physiological models to determine how nonlinear force energetics emerge across molecular, muscular, and whole-body scales.

In conclusion, we show that metabolic energy cost scales superlinearly with both force and force rate, and that this simple power-law relation predicts human force production across muscles, joints, limbs, and fingers. Together with complementary mechanistic modeling, mathematical analysis, and prospective behavioral experiments, these results identify nonlinear metabolic cost as an important principle linking muscle physiology, biomechanics, and sensorimotor control, while providing a quantitative framework for future biomechanical simulations and metabolic estimators[39,40].

Methods

All experiments were approved by the Ohio State University Institutional Review Board and participants took part with informed consent.

Experiment 1: Metabolic cost of time-varying forces. We estimated the metabolic cost of producing time-varying forces as participants tracked target forces using their right leg pressing a force platform while seated comfortably (Figure 2A). Metabolic rate was estimated from respiratory gas exchange (MGC Ultima CardiO2 cart) using $\dot{E} = 16.58\dot{V}CO_2 + 4.51\dot{V}O_2$ W/kg[41]. Trials lasting 5 minutes allowed steady-state metabolic cost. Leg forces perpendicular to the platform were recorded (Vernier) and displayed in real time for feedback in addition to the desired force. Participants tracked periodic piecewise sinusoidal forces, combining two sinusoids with equal means and amplitudes, but potentially different periods t_1 and t_2, so as to have different rise and fall times, $t_1/2$ and $t_2/2$, respectively (Figure 2B and *Supplementary Appendix*).

Participants ($N = 11$ participants, 7 male, 4 female; height = 1.67 $\pm$ 0.18 m; mass 74.45 $\pm$ 27.54 kg; age = 27 $\pm$ 8 years, mean $\pm$ 2 s.d.) completed about 30 trials across two sessions, generating 297 unique conditions and nearly 30 hours of data (two participants completing one session each). Varying t_1 and t_2 produced differing positive and negative force slopes, enabling analysis of cost asymmetries: they were selected such that the total time period $t_{\text{period}} = (t_1 + t_2)/2$ was 1 s, 1.25 s or 1.5 s. The rise time parameter $t_1/2$ was respectively selected from the following three sets: $\{0.125, 0.25, 0.375, 0.5, 0.625, 0.75, 0.875\,\text{s}\}$, $\{0.25, 0.5, 0.75, 1\,\text{s}\}$ and $\{0.25, 0.5, 0.75, 1.0, 1.25\,\text{s}\}$. Mean forces ($F_{\text{mean}}$) were 20%, 35%, 50% of the maximum voluntary force F_{max}, comfortable to sustain over 30 s. Amplitudes (F_{amp}) were 50% and 100% of the mean. Trials were randomized across conditions. Before each trial, we estimated the force from the participants' passive and relaxed leg. This passive force was subtracted from desired and applied forces, so that participants controlled only active force output.

Experiment 2: Metabolic cost of a nearly isometric task. We estimated the metabolic cost of nearly isometric forces with experiments in which human participants alternated between quiet standing for some time (T_{stand}) and standing with knees bent for some time (T_{bent}) with each trial lasting 6-7 minutes (Figure 2C). When the participants have their knees bent while being still, the muscles are nearly isometric. We measured volumetric rates of oxygen and carbon dioxide during the trial (Oxycon Mobile) and estimated metabolic cost using the same as earlier[41]). Body movement was measured with a Vicon T20 motion capture system, and the ground reaction forces under each foot were measured with a Bertec instrumented treadmill. Eight participants participated with informed consent. Participants ($N = 8$; height= 1.81 $\pm$ 0.05 m; mass= 77 $\pm$ 11 kg; age= 24 $\pm$ 6 years, 8 male) were provided visual feedback to bend their knees to lower their hip to one of three bent-knee configurations: 85%, 90% 95% of their normal leg length. Three different $T_{\text{stand}}, T_{\text{bent}}$ combinations, namely $\{15\,\text{s}, 5\,\text{s}\}$, $\{10\,\text{s}, 10\,\text{s}\}$, $\{5\,\text{s}, 15\,\text{s}\}$ with three prescribed knee-bend heights gave nine trials per participant. We also measured the cost of quiet standing ($\dot{E}_{\text{stand}}$) before the trials.

Power law metabolic model for time-varying forces. We hypothesize a metabolic cost model wherein the metabolic cost is a power law function of the joint torque (τ^{γ_1}) and rate of change of torque (torque rate $\dot{\tau}^{\gamma_2}$). We further hypothesize that the metabolic cost of increasing the torque (positive torque rate, i.e., $\dot{\tau} > 0$) can be different from decreasing the torque (negative torque rate, i.e., $\dot{\tau} < 0$). In practice, we fit the following piecewise joint torque based metabolic cost model with joint torque represented in terms of measured external force F_{ext} and positive and negative force rates ($(\dot{F}_{\text{ext}})_{\text{pos}}$ and $(\dot{F}_{\text{ext}})_{\text{neg}}$):

$$\dot{E}_{\text{model}} = a_0 + a_1 F_{\text{ext}}^{\gamma_1} + a_2 (\dot{F}_{\text{ext}})_{\text{pos}}^{\gamma_2} + a_3 (\dot{F}_{\text{ext}})_{\text{neg}}^{\gamma_2}. \tag{4}$$

Limb mass is accounted for by considering the active muscle force production only, subtracting the passive force due to gravity in computing the external force F_{ext}. This external force is proportional to the joint torque from a sagittal plane limb model with a single joint $\tau = \text{constant} \cdot F_{\text{ext}}$ and, as shown elsewhere in this manuscript, this external force is also proportional to individual joint torques in a multi-joint model due to the linear mechanical constraints in isometric tasks. Using all 297 participant trials of experiment 1, we fit the metabolic cost model (equation 1) to the measured metabolic cost ($\dot{E}_{\text{trial}}$) to estimate participant-specific offsets a_0 and coefficients and exponents ($a_1, a_2, a_3, \gamma_1,$ and γ_2) common across all participants by minimizing the mean squared residual across all trials and participants. For each trial, we estimated force rate $\dot{F}_{\text{ext}}$ by using a forward difference approximation, and obtained averages of the external force F_{ext}, and the positive and negative parts of the force rates $(\dot{\text{F}}_{\text{ext}})_{\text{pos}}$ and $(\dot{\text{F}}_{\text{ext}})_{\text{neg}}$ over 150 to 300 s. We normalize the forces by 100 N, force-rates by 100 Ns^{-1}, and second derivatives of force by 100 Ns^{-2}, and all expressed in these normalized units. We estimate metabolic cost for each trial ($\dot{\text{E}}_{\text{trial}}$) as the average over 180 to 300 s, normalized by participant mass. We assume participant specific offsets a_0 to allow for different resting metabolic rates across participants.

Special case: Power law metabolic cost for the nearly isometric task. We fit a metabolic cost model based on ankle, knee and hip joint torques to the experimental data ($\dot{E}_{\text{bent}}$) (Figure 2C). We estimated ankle, knee and hip joint torques through inverse dynamics using the body position and ground reaction force data from the experiment and a sagittal-plane human model with three rigid body segments representing shank, thigh, and upper body with geometric and inertia properties obtained from standard scaling for known participant mass and height[42]. The foot remains motionless in the task, and thus does not contribute to the joint torques. Participants did not keep the knee bends exactly still, and the inverse-dynamics-based torques account for this movement. We hypothesize the special case metabolic cost model: $\dot{E}_{\text{model}} = c_0 + c_1 \tau_{\text{ankle}}^{\gamma_1} + c_2 \tau_{\text{knee}}^{\gamma_1} + c_3 \tau_{\text{hip}}^{\gamma_1}$. Finding that the ankle, knee and hip joint torques as they were highly correlated within a trial (Figure 3C), it was sufficient to fit the equivalent model $\dot{E}_{\text{model}} = b_0 + b_1 (\tau_{\text{ankle}}^{\gamma_1} + \tau_{\text{knee}}^{\gamma_1} + \tau_{\text{hip}}^{\gamma_1})$ to the experimental data ($\dot{E}_{\text{bent}}$); we estimated a single exponent γ_1 common to all participants and participant-specific coefficients b_0 and b_1.

Mechanistic model of muscle energetics. To investigate physiological mechanisms underlying the experimentally observed nonlinear metabolic cost, we developed a mechanistic muscle model incorporating motor-unit recruitment, calcium release and buffering, SERCA-mediated calcium pumping, and force production. Total metabolic energy expenditure was computed as the sum of calcium pumping costs and actomyosin interaction costs during simulated contractions over a range of excitation levels. Complete equations, parameter values, and ablation analyses are provided in Supplementary Section S1.1.

Analytical model of pennation-induced nonlinearity. We derived an analytical model to determine whether muscle pennation alone could generate nonlinear relations between tendon force and metabolic cost. Assuming linear energetic cost at the muscle-fiber level together with force-dependent pennation arising from tendon elasticity and constant muscle volume, we obtained a Taylor-series approximation for whole-muscle metabolic cost as a function of tendon force. The complete derivation is provided in Supplementary Section S1.2.

Comparison with prior metabolic models. To compare our experimentally derived power-law metabolic model with previous formulations, we implemented a muscle-driven leg model with Hill-type muscle–tendon units and estimated metabolic expenditure using the Umberger, Bhargava, and Alexander–Minetti metabolic models, as well as tendon mechanical work. Predictions were compared with experimentally measured metabolic rates across all trials. Model details are provided in Supplementary Section S2.1.

Experiments 3 and 4: Human behavior in bilateral force sharing between arms or legs. We performed bilateral limb force sharing experiments in which human participants track a composite goal force using visual feedback with their two arms ($N_{\text{subjects}} = 12$, 5M, 7F; height = 1.69 $\pm$ 0.11m; mass = 68.83$\pm$ 2.5 kg; age = 20.66$\pm$2.5 years; all right dominant) or two legs ($N_{\text{subjects}} = 21$, 14M, 7F; height = 1.72 $\pm$ 0.08m; mass = 68.1$\pm$10.22 kg; age = 23.6$\pm$4.82 years; mean$\pm$s.d; all right dominant). The composite goal force F_{goal} was a linear combination of the left and the right force: $F_{\text{output}} = \lambda F_{\text{left}} + (1-\lambda) F_{\text{right}}$ (Figure 4B), as used in some previous studies[28,29,43], and tracked for 3 mins. We had different setup configurations for upper and lower limb experiments to measure right and left limb forces (F_{right}, F_{left}) using force plates (Bertec, Vernier, respectively). Participants experienced seven different left-right force contributions ($\lambda = \{0, 0.1, 0.3, 0.5, 0.7, 0.9, 1\}$) with two different goal

force levels which were a fraction (40 and 70%) of maximum limb force ($F_{\max}$) resulting in 14 trials per participant. The maximum limb force $F_{\max}$ was estimated from a 30 s trial where the participants were instructed to apply a maximum force which could be held comfortably using both their limbs and averaging the second half of the trial (15-30 s). For each trial, participants were told which side contributes more to the output for each trial but not the exact value of λ. For lower limbs, we measured the forces when the limbs were resting on the force plates and subtracted it from the individual limb force during the trial to account for forces produced by just muscles.

Minimizing metabolic cost to predict bilateral limb sharing. We expressed metabolic energy cost as a power law function of joint torque (τ^{γ_1}) with exponent γ_1 derived from the energy cost measurements. Our metabolic cost expression for force sharing becomes: $\tau_{\text{right}}^{\gamma_1} + \tau_{\text{left}}^{\gamma_1}$, as we represented each limb using a single joint and rigid segment in the sagittal plane (*Supplementary Appendix*), equivalent to a multi-joint multi-muscle limb as shown in the theorem and its corollaries in the Results. We expressed joint torque in terms of the force applied by each limb ($F_{\text{left}},\ F_{\text{right}}$) on the force plate resulting in the following expression (see *Supplementary Appendix* for derivation):

$$\text{Metabolic cost } = (\text{F}_{\text{left}} - \beta_{\text{left}})^{\gamma_1} + (\text{F}_{\text{right}} - \beta_{\text{right}})^{\gamma_1} \tag{5}$$

β_{left}, and β_{right} were participant specific parameters representing the passive forces exerted by the limbs on the force plates due to gravity that is when the muscles are turned off entirely. We estimated this from model fit to experimental data.

Bilateral limb force sharing: Minimizing error cost. We sought to test whether minimizing error could explain force sharing. Error has two components: systematic error and random error. Systematic error represents the difference between the desired force and the average force tracked by the participant. In our experiments, this difference was close to 1 to 3% due to excellent force tracking by the participants (Figure 4F). So we neglect this systematic error and focus on the random error. The random error is signal dependent, in particular, the standard deviation of a limb force is proportional to the mean force exerted[19], say with proportionality k. In our experiment, the visually observed force output is $\lambda\ F_{\text{left}} + (1-\lambda)\ F_{\text{right}}$, containing the two terms $\lambda\ F_{\text{left}}$ and $(1-\lambda)\ F_{\text{right}}$. Since F_{left} and F_{right} consist of passive component due to gravity which is not signal dependent, we consider only active part of the force which is $(F_{\text{left}} - \beta_{\text{left}})$ and $F_{\text{right}} - \beta_{\text{right}})$. Putting all this together, the variance of the observed force output $\lambda\ F_{\text{left}} + (1-\lambda)\ F_{\text{right}}$ is given by the following expression:

$$\text{Error cost } = \lambda^2(\text{F}_{\text{left}} - \beta_{\text{left}})^2 + (1-\lambda)^2(\text{F}_{\text{right}} - \beta_{\text{right}})^2. \tag{6}$$

Bilateral limb force sharing: Trade-off between metabolic cost and error We sought to test if the participants minimized some mixture of effort and variability during force sharing. Hence, we considered an additive cost, representing a trade-off between metabolic and variability given by the following expression: δ Metabolic cost $+(1-\delta)$ Error cost, with parameter δ estimated from model fit to experiment.

Using the cost functions described above, we performed constrained optimisation with the constraint posed in the experiment ($\alpha F_{\max} = \lambda F_{\text{left}} + (1-\lambda)F_{\text{right}}$) to predict the left and right limb force for all experimental trials for a given value of model unknowns β_{left}, β_{right} and δ (for model 3). We estimated the optimum model unknowns by minimizing the mean squared residual with the experiment. We then used these cost functions to predict human behaviour for non-experimental force sharing conditions for upper and lower limb separately. In addition to the predictions from the metabolically derived γ, we also performed additional optimizations to obtain the γ that best fit the experiments.

Finger force sharing: bimanual and unimanual. For bimanual force sharing between analogous and non-analogous fingers identically to bilateral force sharing between limbs, except that the 'limbs' are now fingers, with the two fingers having unknown coefficients premultiplying their corresponding term, so that the cost becomes: $\alpha_{\text{left}}(F_{\text{left}} - \beta_{left})^{\gamma_1} + \alpha_{\text{right}}(F_{\text{right}} - \beta_{\text{right}})^{\gamma_1}$. For unimanual finger force sharing with four fingers, the cost now has N such terms instead of two, where each term corresponds to one effective muscle: $\sum_{i=1}^{N} \alpha_i (G_i)^{\gamma_1}$, where G_i are the muscle forces and α_i are unknown coefficients; the passive finger forces β are negligible. Each muscle potentially actuates multiple fingers, with the individual finger forces $F = [F_1; \ldots; F_4]$ being linear transformations of these effective muscle forces: $F = AG$, where A is an unknown linear transformation. We infer the unknown constants to best fit the experimental data; we found four muscles sufficient to capture the observed behavioral data, while fewer muscles had more error in reproducing the data and more muscles did not improve accuracy.

Optimal feedback control. For the two-limb force sharing task, the unknowns of the optimal feedback control problem consisted of the feedback control policy, which was parameterized by the mean forces on the two limbs and the feedback gains that transform the task error to limb force. We solved for these unknowns using a nonlinear constrained optimization procedure so as to minimize a cost function integrated over the task duration subject to the task constraint of meeting the target goal force (as a linear combination of the two limb forces) averaged over the task duration, both objective and constraints averaged over multiple realizations of signal dependent motor noise. The limb force returned by the feedback controller are rectified

to be positive. The cost function was had two terms summed linearly: metabolic energy cost and goal force variance, whose weightings are obtained empirically. The metabolic energy cost has the nonlinear force and force-rate terms as obtained in our metabolic experiments, so that both large forces and force-rates are penalized.

References

1. Alexander, R. M. Optimization and gaits in the locomotion of vertebrates. *Physiol. reviews* **69**, 1199–1227 (1989).
2. Srinivasan, M. Optimal speeds for walking and running, and walking on a moving walkway. *Chaos: An Interdiscip. J. Nonlinear Sci.* **19** (2009).
3. Huang, H. J., Kram, R. & Ahmed, A. A. Reduction of metabolic cost during motor learning of arm reaching dynamics. *J. Neurosci.* **32**, 2182–2190 (2012).
4. Brown, G. L., Seethapathi, N. & Srinivasan, M. A unified energy-optimality criterion predicts human navigation paths and speeds. *Proc. Natl. Acad. Sci.* **118**, e2020327118 (2021).
5. Seethapathi, N. & Srinivasan, M. The metabolic cost of changing walking speeds is significant, implies lower optimal speeds for shorter distances, and increases daily energy estimates. *Biol. letters* **11**, 20150486 (2015).
6. Long III, L. L. & Srinivasan, M. Walking, running, and resting under time, distance, and average speed constraints: optimality of walk–run–rest mixtures. *J. The Royal Soc. Interface* **10**, 20120980 (2013).
7. Selinger, J. C., O'Connor, S. M., Wong, J. D. & Donelan, J. M. Humans can continuously optimize energetic cost during walking. *Curr. Biol.* **25**, 2452–2456 (2015).
8. Wong, J. D., Cluff, T. & Kuo, A. D. The energetic basis for smooth human arm movements. *Elife* **10**, e68013 (2021).
9. Paul, R. J. & Peterson, J. W. Relation between length, isometric force, and o2 consumption rate in vascular smooth muscle. *Am. J. Physiol. Content* **228**, 915–922 (1975).
10. Hood, D. A., Gorski, J. & Terjung, R. L. Oxygen cost of twitch and tetanic isometric contractions of rat skeletal muscle. *Am. J. Physiol. Metab.* **250**, E449–E456 (1986).
11. Glück, E. & Paul, R. J. The aerobic metabolism of porcine carotid artery and its relationship to isometric force. energy cost of isometric contraction. *Pflugers Arch. Eur. J. Physiol.* **370**, 9–18 (1977).
12. Clarke, D. H. Energy Cost of Isometric Exercise. *Res. Quarterly. Am. Assoc. for Heal. Phys. Educ. Recreat.* **31**, 3–6 (1960).
13. Royce, J. Oxygen intake curves reflecting circulatory factors in static work. *Int. Zeitschrift fur angewandte Physiol. einschliesslich Arbeitsphysiologie* **19**, 222–228 (1962).
14. Umberger, B. R., Gerritsen, K. G. & Martin, P. E. A model of human muscle energy expenditure. *Comput. methods biomechanics biomedical engineering* **6**, 99–111 (2003).
15. Huxley, A. F. Muscle structure and theories of contraction. *Prog. biophysics biophysical chemistry* **7**, 255–318 (1957).
16. Zahalak, G. I. Modeling muscle mechanics (and energetics). *Multiple muscle systems: biomechanics movement organization* 1–23 (1990).
17. Bhargava, L. J., Pandy, M. G. & Anderson, F. C. A phenomenological model for estimating metabolic energy consumption in muscle contraction. *J. biomechanics* **37**, 81–88 (2004).
18. Kuroda, E., Klissouras, V. & Milsum, J. Electrical and metabolic activities and fatigue in human isometric contraction. *J. Appl. Physiol.* **29**, 358–367 (1970).
19. Harris, C. M. & Wolpert, D. M. Signal-dependent noise determines motor planning. *Nature* **394**, 780–784 (1998).
20. Alwan, A. & Srinivasan, M. Natural variability increases human walking metabolic costs and its implications to simulation-based metabolic estimation. *bioRxiv* (2025).
21. van der Zee, T. J. & Kuo, A. D. The high energetic cost of rapid force development in muscle. *J. Exp. Biol.* **224**, jeb233965 (2021).
22. Hawkins, D. & Molé, P. Modeling energy expenditure associated with isometric, concentric, and eccentric muscle action at the knee. *Annals biomedical engineering* **25**, 822–830 (1997).
23. O'Sullivan, I., Burdet, E. & Diedrichsen, J. Dissociating variability and effort as determinants of coordination. *PLoS computational biology* **5**, e1000345 (2009).
24. Todorov, E. & Jordan, M. I. Optimal feedback control as a theory of motor coordination. *Nat. neuroscience* **5**, 1226–1235 (2002).

25. Hu, X. & Newell, K. M. Visual information gain and task asymmetry interact in bimanual force coordination and control. *Exp. brain research* **212**, 497–504 (2011).

26. Jin, Y., Kim, M., Oh, S. & Yoon, B. Motor control strategies during bimanual isometric force control among healthy individuals. *Adapt. Behav.* **27**, 127–136 (2019).

27. Hu, X. & Newell, K. M. Modeling constraints to redundancy in bimanual force coordination. *J. Neurophysiol.* **105**, 2169–2180 (2011).

28. Hu, X. & Newell, K. M. Adaptation to bimanual asymmetric weights in isometric force coordination. *Neurosci. letters* **490**, 121–125 (2011).

29. Nathaniel Skinner. *Subjective costs of movement*. Ph.D. thesis, University of Michigan (2014).

30. Fagg, A. H., Shah, A. & Barto, A. G. A computational model of muscle recruitment for wrist movements. *J. Neurophysiol.* **88**, 3348–3358 (2002).

31. Burdet, E. & Milner, T. E. Quantization of human motions and learning of accurate movements. *Biol. cybernetics* **78**, 307–318 (1998).

32. Valero-Cuevas, F. J. Predictive modulation of muscle coordination pattern magnitude scales fingertip force magnitude over the voluntary range. *J. Neurophysiol.* **83**, 1469–1479 (2000).

33. Morrison, S. & Newell, K. Interlimb coordination as a function of isometric force output. *J. Mot. Behav.* **30**, 323–342 (1998).

34. Zatsiorsky, V. M., Li, Z.-M. & Latash, M. L. Coordinated force production in multi-finger tasks: finger interaction and neural network modeling. *Biol. cybernetics* **79**, 139–150 (1998).

35. Josenhans, W. T. Muscular factors. *Can. Med. Assoc. J.* **96**, 761–764 (1967).

36. Cerretelli, P., Veicsteinas, A., Fumagalli, M. & Dell'Orto, L. Energetics of isometric exercise in man. *J. applied physiology* **41**, 136–141 (1976).

37. Erdemir, A., McLean, S., Herzog, W. & van den Bogert, A. J. Model-based estimation of muscle forces exerted during movements. *Clin. biomechanics* **22**, 131–154 (2007).

38. Terekhov, A. V., Pesin, Y. B., Niu, X., Latash, M. L. & Zatsiorsky, V. M. An analytical approach to the problem of inverse optimization with additive objective functions: an application to human prehension. *J. mathematical biology* **61**, 423–453 (2010).

39. Annerino, A., Faltas, M., Srinivasan, M. & Gouma, P.-I. Towards skin-acetone monitors with selective sensitivity: Dynamics of pani-ca films. *Plos one* **17**, e0267311 (2022).

40. Khusainov, R., Azzi, D., Achumba, I. E. & Bersch, S. D. Real-time human ambulation, activity, and physiological monitoring: Taxonomy of issues, techniques, applications, challenges and limitations. *Sensors* **13**, 12852–12902 (2013).

41. Brockway, J. Derivation of formulae used to calculate energy expenditure in man. *Hum. nutrition. Clin. nutrition* **41**, 463–471 (1987).

42. De Leva, P. Adjustments to zatsiorsky-seluyanov's segment inertia parameters. *J. biomechanics* **29**, 1223–1230 (1996).

43. Ambike, S., Zatsiorsky, V. M. & Latash, M. L. Processes underlying unintentional finger-force changes in the absence of visual feedback. *Exp. brain research* **233**, 711–721 (2015).

Acknowledgements

This work was supported by NIH-R01GM135923 and NSF SCH grant 2014506. Thanks to the Ohio State CRC for access to metabolic testing.

Author contributions statement

S.S.M., N.M., C.M., and M.S contributed to study conception and experiment design. S.S.M, N.M, and C.M. performed most experiments. S.S.M. and N.M. performed data analyses. S.S.M. and M.S. proved the theorem. H.X.R. and S.W. suggested additional analyses. Z.W. and A.A. performed some experiments and data analyses. R.B. contributed to instrumentation design. K.H. contributed materials and to experiments. S.S.M. and N.M. wrote initial drafts; S.S.M., N.M., H.X.R. S.W. and M.S. helped revise the manuscript. S.S.M. contributed equally to this work with N.M.

Supplementary Appendix for: Energy cost for force is nonlinear and predicts human forces in legs, arms, fingers, and muscles

Sriram Sekaripuram Muralidhar[1,5,*,+], Nadja Marin[1,+], Colin Melick[1], Hansol X Ryu[1], Aya Alwan[1], Zhengcan Wang[1], Ross Baldwin[1], Kristen Heitman[1], Sam Walcott[4], and Manoj Srinivasan[1,2,3,*]

[1]Mechanical and Aerospace Engineering, The Ohio State University, Columbus OH 43201
[2]Program in Biophysics, The Ohio State University, Columbus OH 43201
[3]Ecology, Evolution, and Organismal Biology, Brown University, Providence RI 43201
[4]Mathematical Sciences, and Bioinformatics and Computational Biology, Worcester Polytechnic Institute, Worcester MA01609
[5]Biokinesiology and Physical Therapy, University of Southern California, Los Angeles CA 90007
[6]Health and Rehabilitation Sciences, The Ohio State University, Columbus OH 43201
[*]srirammu@usc.edu; srinivasan.88@osu.edu
[+]these authors contributed equally to this work

ABSTRACT

This is a Supplementary Appendix, containing additional technical details of methods and mathematical theorems.

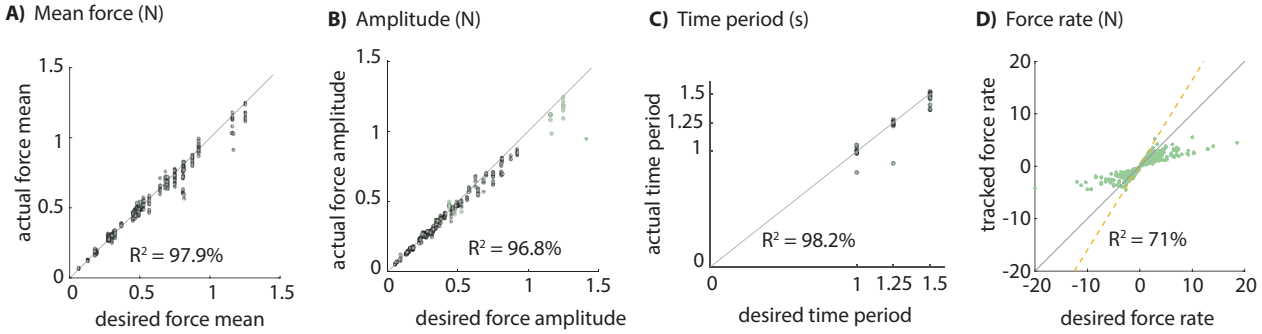

Figure S1. Subjects' tracking of target forces. Tracked quantities obtained by averaging the entire 5 mins of time-series data. **A)** Piecewise sinusoid means (F_{mean}) are tracked well by subjects. **B)** Piecewise sinusoid amplitudes (F_{amp}) are tracked well by subjects. **C)** Piecewise sinusoid time-periods ($t_{period} = (t_1 + t_2)/2$) are tracked well by subjects **D)** The effective mean positive and negative force-rates across trials are imperfectly tracked by the subjects.

S1 Models of energy versus force nonlinearity

S1.1 Energetics of force production with motor unit recruitment, calcium, and force dynamics.

We obtained nonlinear dependence of muscle energetics with force by simulating a muscle with a large number of motor units, wherein each motor unit is recruited based on the size principle and is stimulated with firing rate that increases with overall excitation. Each motor unit had a simplified model of calcium and force dynamics, allowing us to estimate the total energy cost of force production due to two sources: myofibrillar interaction and calcium pumping by the SERCA pump back into the sarcoplasmic reticulum.

Each motor unit has four dynamical state variables: concentration of free (unbound) calcium C_f, concentration of calcium bound to a calcium buffer C_b (e.g., parvalbumin), motor unit force F, and the release availability of calcium from the

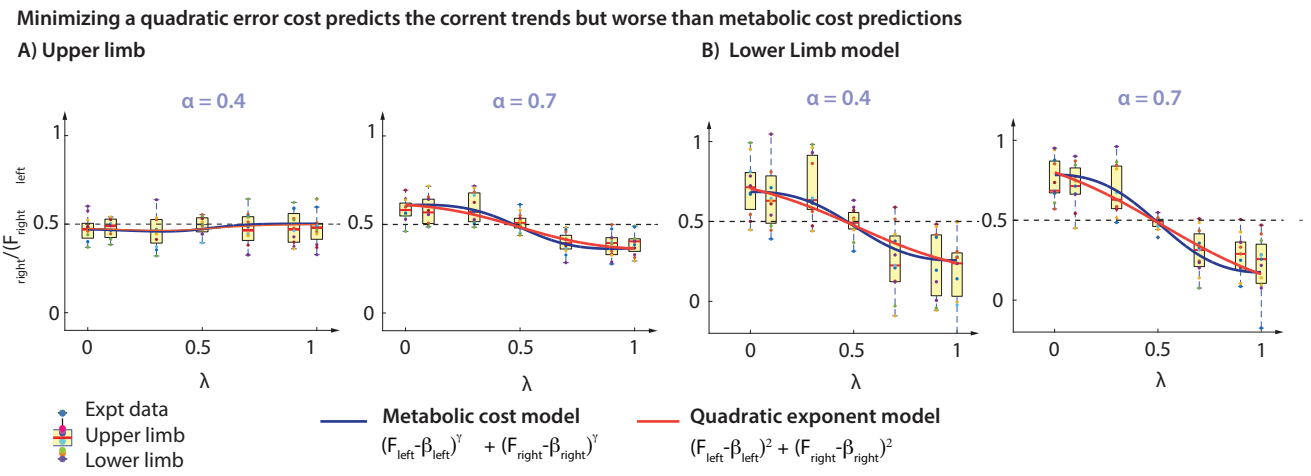

Figure S2. How good is a quadratic model. A quadratic cost model is similar to but slightly worse than the metabolic cost model in explaining the data (Upper limb: RMSE = 0.4953, R^2 = 72.61%; Lower limb: RMSE =1.291, R^2 =76.85%).

sarcoplasmic reticulum q. The equations governing these variables are as follows:

$$\frac{dC_f}{dt} = R(t) - J_{\text{SERCA}}(C_f) - k_b C_f\,(B_{\text{total}} - C_b) + k_u C_b \tag{1}$$

$$\frac{dC_b}{dt} = k_b C_f\,(B_{\text{total}} - C_b) - k_u C_b \tag{2}$$

$$\frac{dF}{dt} = \frac{1}{\tau_F}\left(\Phi(C_f) - F\right) \tag{3}$$

$$\frac{dq}{dt} = \frac{(1-q)}{\tau_q} \tag{4}$$

where τ_F is the time constant of force dynamics given free calcium, and τ_q is the time-constant with which the release availability q is replenished.

Equation 1 represents the dynamics of free calcium with calcium release from the sarcoplasmic reticulum $R(t)$, the pumping of free calcium back into the sarcoplasmic reticulum $J_{\text{SERCA}}(C_f)$, binding of free calcium with the buffer $k_b C_f\,(B_{\text{total}} - C_b)$, and the release of free calcium from the buffer $k_u C_b$; here, B_{total} is the total buffer available, and k_b and k_u are constant reaction rates of calcium binding and unbinding to the buffer. The SERCA pump rate $J_{\text{SERCA}}(C_f)$ is given by the Hill equation:

$$J_{\text{SERCA}}(C_f) = V_{\max}\frac{C_F^m}{K_S^m + C_f^m}, \tag{5}$$

where $V_{\max}$ is the maximum pumping rate. The total energy cost of force production is obtained as the sum of the energy cost of this calcium pumping to the cost of actin-myosin interaction, assumed linear in force produced:

$$E_{\text{total}} = 0.5\int_0^T J_{\text{SERCA}}\,dt + \int_0^T b_F\,F\,dt \tag{6}$$

where the 0.5 factor in the first term represents one ATP per two calcium ions transported by SERCA.

Equation 2 represents the dynamics of calcium bound to the buffer, just containing two terms, binding of calcium to the buffer and the unbinding. Equation 3 implicitly models activation via troponin and tropomyosin and force production via actin-myosin cycling. The function $\Phi(C_f)$ relates the steady state motor unit force to the free Calcium in the myofibrillar space and is given by the following Hill equation:

$$\Phi(C_f) = F_{\max}\frac{C_F^m}{K_F^m + C_f^m}, \tag{7}$$

where $F_{\max}$ is the maximum possible motor unit force.

Equation 4 represents the dynamics of the variable q, which models the calcium release availability of the sarcoplasmic reticulum, determining how much calcium is released upon a neural spike. The function $R(t)$ indicating calcium release is zero between neural spikes; each neural spike stimulating the motor unit results in the release of calcium into the myofibrillar space, increasing the free calcium concentration as follows:

$$C_f(t^+) - C_f(t^-) = Aq(t^-), \tag{8}$$

where the state variable q models the various refractory processes that limits release availability of calcium soon after a spike; t^+ and t^- represent time t just before and after a neural spike. This release availability variable q is depleted by each neural spike as follows: $q(t^+) = q(t^-)(1-\alpha)$, with $0 < \alpha < 1$ and gets replenished slowly via equation 4.

To scale up this single motor unit dynamics to a full muscle, we adapt a simplified model of motor unit recruitment and rate coding of motor unit force[1]. We consider $N_{\mathrm{MU}} = 120$ motor units, each with $F_{\max}$ given by:

$$F_{\mathrm{max,j}} = e^{bj}, \tag{9}$$

where the forces are in some arbitrary units and the variable j indexes the motor units from 1 to 120 in increasing order of size and force. The time constant of force dynamics tau_F for each motor unit is inversely related to this force by the following relation:

$$\tau_{F,j} = T_L \left(\frac{1}{F_{\mathrm{max,j}}} \right)^{c^{-1}}. \tag{10}$$

The muscle as a whole receives an excitation signal E, and each motor unit has a threshold at which it starts firing, that is, produces spikes at a minimum firing rate (MFR). The recruitment thresholds increase with motor unit size per the size principle, modeled by the following relation:

$$RTE_j = e^{aj}. \tag{11}$$

When the threshold is exceeded, the firing rate FR increases linearly for each motor unit as follows:

$$FR = MFR + g_e \cdot (E - RTE_j), \tag{12}$$

until a peak firing rate is reached; the peak firing rate is smaller for larger units as follows:

$$PFR_j = PFR_1 - PFRD \cdot RTE_j / \max_j(RTE_j). \tag{13}$$

The firing rate FR determines the interspike interval ISI = 1/FR, and this interspike interval has some random variability with some coefficient of variation ($\mathrm{cv_{ISI}}$). This recruitment model is identical to the Fuglevand model, except that the Fuglevand model[1] did not have calcium or buffer dynamics, but directly translated spikes to forces via second order dynamics.

To sum energy costs across motor units, we scale the SERCA pumping rate for each motor unit by the motor unit's cross sectional area, or equivalently, $F_{\mathrm{max,j}}$. We incorporate the presence of two types of motor units, slow-twitch and fast-twitch as follows: (1) the fast-twitch muscles have faster SERCA pump isoforms, so we assume a factor of 2 in the maximum pump rate $V_{\max}$; (2) the fast-twitch muscles have faster myosin isoforms resulting in higher cycling rates, so we assume a factor of 2 in the energy cost of force b_F; (3) the fast-twitch muscles have slightly lower K_S by about 10%. We simulated the muscle for about 4 seconds for a range of excitation levels, and extracted the steady state force and metabolic energy rates: the resulting relation was well-fit by a power law with exponent $\gamma_1 = 1.49$, reminiscent of our experimental measurements. Model parameters used are provided in Table S2, but one can use a wide range of model parameters that result in the same qualitative nonlinearity. Further, ablation studies reveal that the model contains multiple features that lead to nonlinearity between force and energy cost; we systematically ablated one or more model features and found that the nature of the nonlinearity changed, becoming weaker (more commonly) or stronger (in one case). See figure S6.

S1.2 How pennation can add to the nonlinearity.

We asked whether pennation alone can make whole-muscle metabolic cost increase nonlinearly with muscle-tendon force, even if energetic cost is exactly linear in individual muscle fibers. Assume that fiber metabolic cost is proportional to fiber force, $\dot{E} = k_e F_f$, and the tendon force[1] satisfies $F_t = F_f \cos\theta$, where θ is the pennation angle.

When muscle fibers produce force without skeletal movement, the tendon stretches and the muscle fibers shorten and rotate, so that the pennation angle θ becomes an increasing function of force F_f. Specifically, if the total muscle-tendon length is fixed

[1] Of course, by 'tendon', we mean tendon, aponeuroses and any other connective tissue that form the series elastic element.

and the tendon is linear elastic with stiffness k_t, the tendon stretch due to force F_t is F_t/k_t; the projection of the fascicle along the tendon direction will decrease by F_t/k_t, so that this projected fascicle length will be:

$$x_f = L_{f0}\cos\theta_0 - fracF_tk_t = L_f\cos\theta, \tag{14}$$

where the initial projected length before stretch is $L_{f0}\cos\theta_0$. The constant muscle volume condition gives $L_f\sin\theta = L_{f0}\sin\theta_0$. Solving for θ, we get

$$\theta = \tan^{-1}\frac{L_{f0}\sin\theta_0}{L_{f0}\sin\theta_0 - F/k_t}. \tag{15}$$

Substituting this expression and the fiber force expression $F_f = F_t/\cos\theta$ into the energy cost expression $\dot{E} = k_eF_f$, and doing a two-term Taylor series expansion in tendon force gives the following expression for the metabolic rate:

$$\dot{E} \approx k_e\sec\theta_0 F_t + k_e\frac{\tan^2\theta_0}{k_tL_{f0}}F_t^2. \tag{16}$$

The nonlinear coefficient scales like $\tan^2\theta_0$, so the pennation-induced nonlinearity is small for small pennation angles but rises quickly for highly pennate muscles. The presence of linear and quadratic term in the Taylor series suggests good approximation by a power law with exponent between 1 and 2.

S2 Computations with a muscle-driven model of a leg

To estimate muscle mechanical work and to estimate metabolic cost using prior metabolic models, we use a muscle-driven model of the leg[2–4]. The muscle properties are listed in table S1: eight consolidated muscles with constant moment arms, both uniarticular and biarticular, applying torques about one or more of the hip, knee, and ankle joints.

S2.1 Prior metabolic costs.

The list of joint torques τ are given by: $\tau = -J^TF_{\text{ext}}$, where J is the Jacobian of the ankle position relative to the joint angles and F_{ext} is the external force. The torques are also equal to the muscle moment arms times the muscle forces, summed: $\tau = DF_m$, where D is the matrix of moment arms as in Table S1. Under changing external forces, we solve for the muscle forces by minimizing just force cost from the main manuscript, as that term dominates the force sharing (and we estimate that the results would not change much by minimizing the force and force-rate cost with an additional work cost, say). Once the muscle forces are solved for, we estimate the amount of work and the corresponding metabolic cost, as well as the other popular metabolic cost models, specifically, the Umberger model, the Bhargava models, and the Alexander-Minetti model[5,6]. See figure S4 for comparison of these model predictions with experimental data: it appears that all the models considered underestimate the experimentally measured metabolic cost.

S2.2 Implications of co-contration.

To simulate co-contraction, we first solved for the cost-optimal muscle force which, by definition, did not have unnecessary muscle activation: specifically, there is no iliopsoas activation (no hip cocontraction). Then, to enforce iliopsoas coactivation, we constrain the iliopsoas force (normalized by F_{iso}) to be a specific fraction (20%) of the normalized glutei force. This proportional scaling was motivated by experimental antagonist EMG observations in van der Zee and Kuo[7]. See figure S5 for results, showing that enforcing cocontraction with these assumptions does not change the optimality of the linear force-sharing strategy, and consequently, the power-law relation for the metabolic rate.

S3 Additional experimental methods

Piecewise sinusoids The piecewise sinusoids tracked by the human participants in metabolic experiment 1 are given by the following equation:

$$F(t) = F_{\text{mean}} + F_{\text{amp}}\cdot\sin\left(\frac{2\pi t}{t_1}\right) \text{ for } 0 \le t < \frac{t_1}{2} \text{ and} \tag{17}$$

$$F(t) = F_{\text{mean}} + F_{\text{amp}}\cdot\sin\left(\frac{2\pi(t-t_1/2)}{t_2}\right) \text{ for } \frac{t_1}{2} \le t < \frac{t_1+t_2}{2}. \tag{18}$$

Muscle name	F_{iso} (N)	k_{tendon} (N/mm)	v_{max} (m/s)	d_{hip} (mm)	d_{knee} (mm)	d_{ankle} (mm)
Iliopsoas	1500	264.1	1.069	50	0	0
Glutei	3000	477.7	2.097	-62	0	0
Hamstrings	3000	224.6	1.090	-72	-34	0
Rectus	1200	75.37	0.8492	34	50	0
Vasti	7000	300	0.9750	0	42	0
Gastrocnemius	3000	178.6	0.5766	0	-20	-53
Soleus	4000	408.2	0.5766	0	0	-53
Tibialis Anterior	2500	0.8597	197.2	0	0	37

Table S1. Muscle-tendon parameters for muscle-driven leg model.

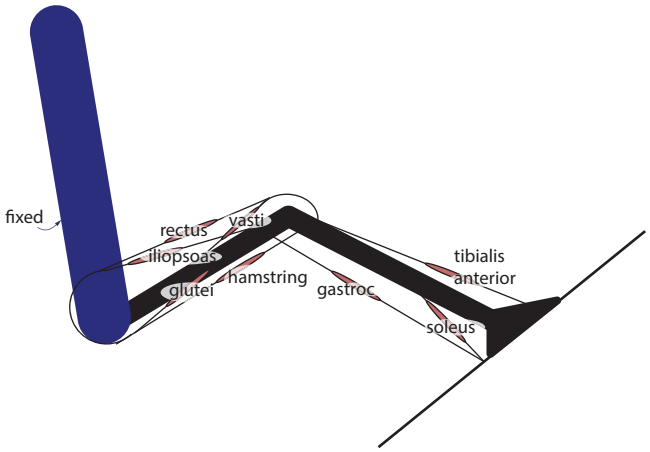

Figure S3. Muscle-driven model of leg[2–4] used to estimate muscle work and metabolic cost based on prior models such as those due to Umberger[5] and Bharagava[6].

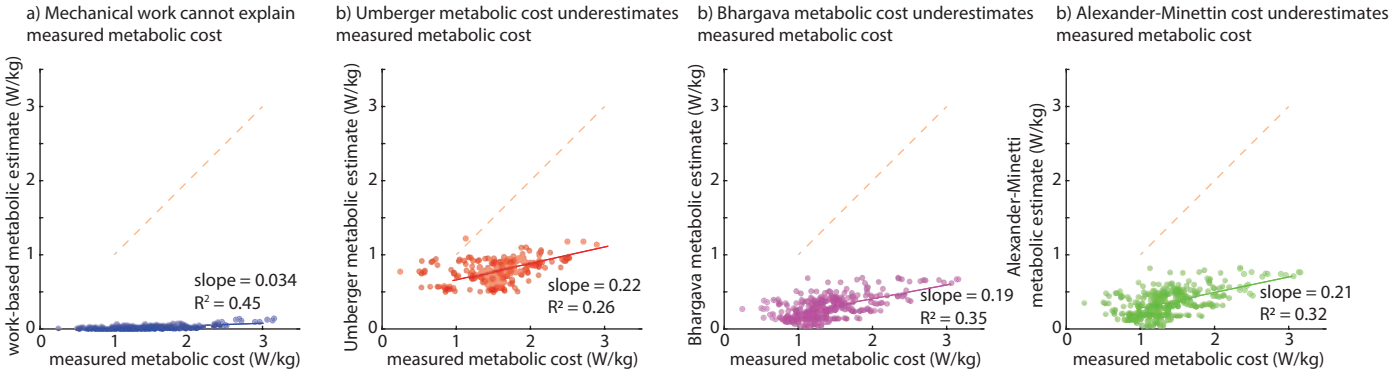

Figure S4. Common metabolic model estimates underestimate measured metabolic cost. a) Mechanical work by muscles due to tendon deformation underestimates the measured metabolic cost, explaining only about 3%. b) Metabolic estimates of the Umberger model[5] are about 22% of the measured cost. c) Metabolic estimates by the Bhargava model are about 19% of the measured cost. d) Metabolic estimates by the Alexander-Minetti model are about 21% of the measured cost. The R^2 values provided indicate how much of the measured metabolic variance can be explained by each model.

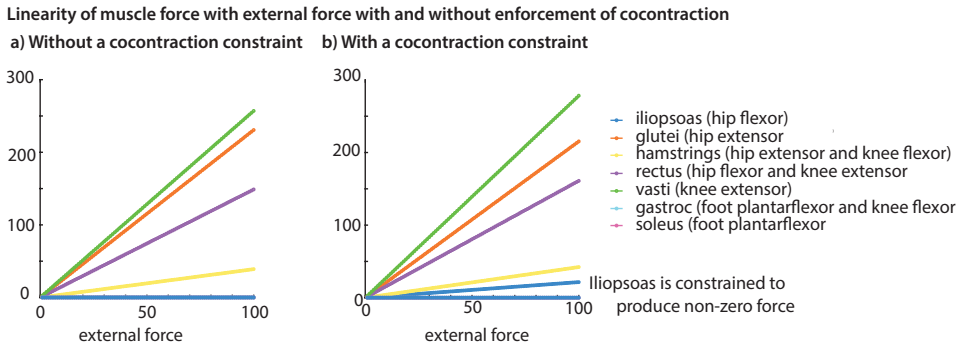

Figure S5. Muscle forces scale linearly when external force is scaled, even in the presence of a co-contraction constraint. a) Muscle forces minimizing the basic power law objective demonstrate in linear scaling with external force. b) Muscle forces minimizing the power law objective but with an additional constraint for the antagonist iliopsoas force to be scaled proportionally to the agonist glutei force. This cocontraction constraint still results in linear scaling of muscle forces with external force.

Accuracy of tracking the desired forces. The participants were reasonable in tracking the desired force means F_{mean}, amplitudes F_{amp}, and the total time period t_p of the piecewise sinusoid ($R^2 > 97\%$ for all of them, Figure S1A, B, C). They were poorer in tracking individual sinusoid rise and fall times $t_1/2$ and $t_2/2$ (see Appendix figure S1), participants preferred individual time periods (t_1 and t_2) closer to symmetry than prescribed. Nevertheless, the actual rise and fall times were correlated enough with the desired times so that we obtained a big diversity of positive and negative force rates highly correlated with the desired force rates (Figure S1D, $R^2 = 71\%$). Because the participants did not track the desired forces with negligible error, all calculations and model predictions use actual forces produced.

Expressing joint torque in terms of external forces on the limb in the cost function. Consider a single segment model of a limb applying an external force, as in Figure S8. The moment balance about the pivot gives: $\tau = L\sin\theta\,(F - mg\,L_{com}/L\,)$. Defining $\beta = mg\,L_{com}/L$, we get $\tau = L\,(F-\beta)\sin\theta$. Substituting this torque expression into the joint-torque-based energy cost function, we get (up to a proportionality constant): $\dot{E} = \tau_{\text{left}}^{\gamma} + \tau_{\text{right}}^{\gamma} = (\text{L}\,\sin\theta)^{\gamma}\left[(\text{F}_{\text{left}} - \beta_{\text{left}})^{\gamma} + (\text{F}_{\text{right}} - \beta_{\text{right}})^{\gamma}\right]$, assuming $\text{L}_{\text{left}} = \text{L}_{\text{right}} = \text{L}$ and $\theta_{\text{left}} = \theta_{\text{right}} = \theta$. For the purposes of optimization with a fixed, static configuration, the constant term $(\text{L}\,\sin\theta)^{\gamma}$ does not matter. So, we have: Cost function $= (F_{\text{left}} - \beta_{\text{left}})^{\gamma} + (F_{\text{right}} - \beta_{\text{right}})^{\gamma}$.

S4 Theorem: Linear scaling strategy for muscle forces and joint torques.

In the main manuscript, we expressed the metabolic cost as a function of external force and force rate, using a single-link model. Now, we consider a limb with multiple joints and multiple muscles. As in our experiment, this limb at rest needs to produce a one-parameter family of external forces and force rates, all along the same direction but of different force and force-rate magnitudes. We now show that if all the muscles power-law metabolic cost, all with the same force exponent and same force rate exponent, the energy optimal muscles forces for the task follow a 'linear scaling strategy.' That is, if the energy optimal solution is known for one external force and force rate magnitude, the optimal solution for any other external force and force rate magnitude is obtained by linearly scaling all the muscle forces by one scalar factor and the force rate magnitudes by a different scalar factor.

S4.1 Static condition without force rate costs

Theorem: Metabolic power law scaling predicts a linear muscle force scaling strategy in a static task. We have framed the power law metabolic cost model thus far as being a function of joint torques or of external force. Here, we generalize the metabolic cost to being a power law function of muscle force and show the self-consistency of power law relations at the level of muscles, joints, and limbs. To show this self-consistency, we first show that a linear scaling strategy for producing external forces is optimal, as seen in experiments[8,9].

Consider the task of producing an external force of different magnitudes but fixed direction using a limb with multiple muscles and multiple joints, when the limb is at rest (Figure S7). We show that minimizing the power law metabolic cost results in a 'linear scaling strategy' for muscle forces, as seen in some finger force experiments[8]. That is, once the optimal solution is determined for one external force magnitude, the optimal solution for any other external force magnitude is simply scaling all the muscle force magnitudes by the same scalar factor. In more detail, consider a task in which a multi-joint (open-chain) limb with m muscles (Figure S7) is at rest and needs to apply a 3D external force $\mathbf{F}_{\text{ext}}$, which is a scaled version $\mu\mathbf{F}_0$ of some

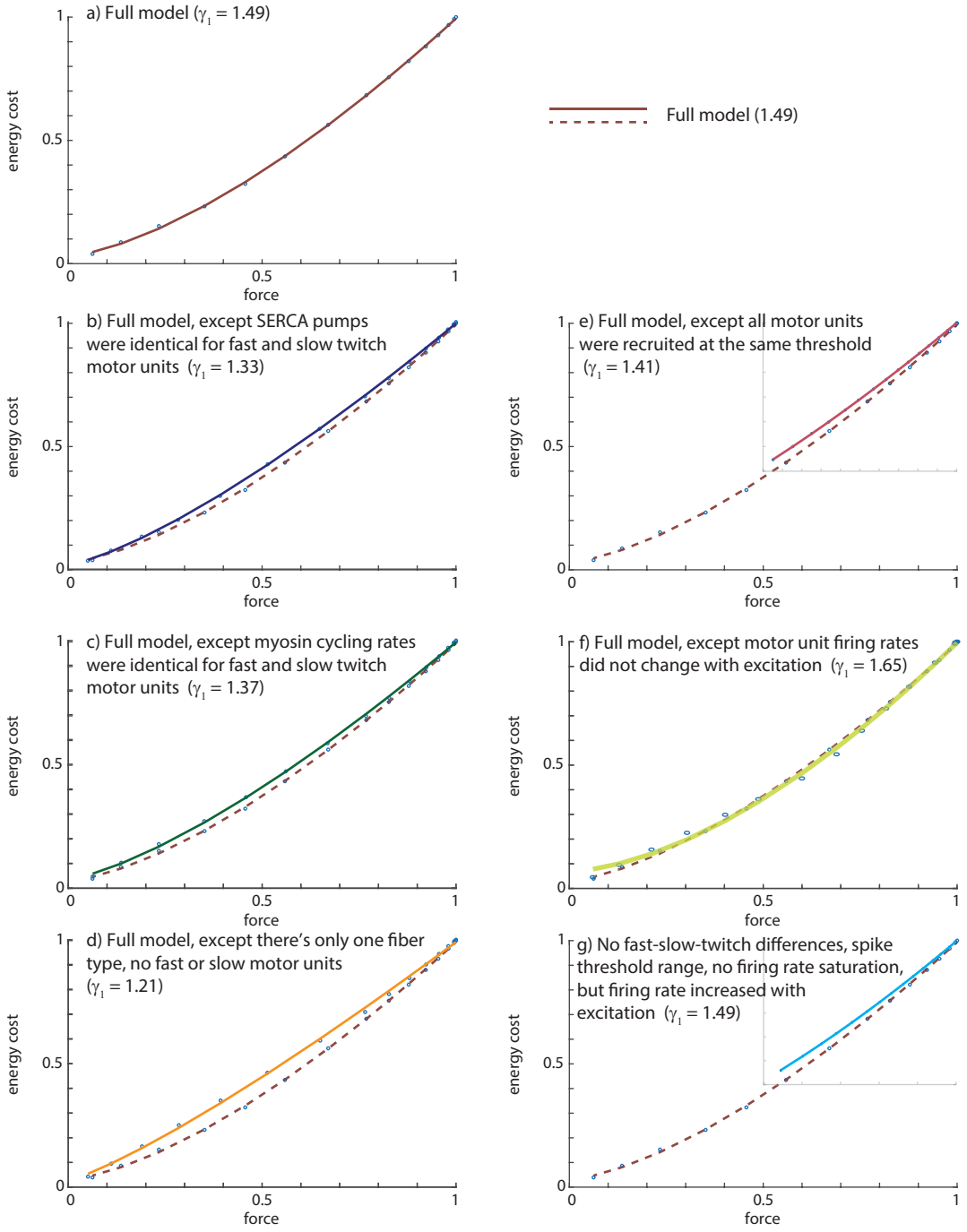

Figure S6. Model with motor unit recruitment, rate coding of force via firing rate increase, calcium and force dynamics, and distinct fast and slow motor units produces nonlinearity reminiscent of our experimental observations. a) Full model containing all the effects. Panels b-g ablate one or more model features to examine if the features contribute to the nonlinearity: it appears all these model features have some effect on the strength of the nonlinearity. The power law exponent γ_1 that best fits each model variant is shown parenthetically. b) Ablation: the SERCA pumps were not different for fast and slow twitch units. c) Ablation: the actomyosin cycling rates were not different for fast and slow twitch units. d) Ablation: only one motor unit type, no fast vs slow motor units. e) Ablation: all motor units recruited at the same threshold, rather than there being orderly recruitment. f) Ablation: motor unit firing rates did not increase with excitation. g) Multiple ablations: no fast vs slow differences, all units recruited at the same threshold, no firing rate saturation; firing rate did increase with excitation. The solution to the full model is shown on every 'ablation' panel for reference as a dashed line, but as a solid line in panel a.

nominal 3D external force $\mathbf{F}_0$, where μ is a positive scalar. Then, if the optimal muscle force magnitudes for the nominal external force $\mathbf{F}_0$ are given by $\mathbf{F}_{\text{mus0}} \in \mathbb{R}^m$, then the optimal muscle force magnitudes for any other external force $\mu\mathbf{F}_0$ are given by $\mu\mathbf{F}_{\text{mus0}}$, assuming the external force is much larger than limb weight due to gravity. In the Supplementary Appendix S4.2, we show a generalization of this theorems and its following corollaries to include time-varying forces including both the force and force-rate costs.

The condition that the whole limb is in static equilibrium is a linear equation in the list of m muscle force magnitudes $\mathbf{F}_{\text{mus}} \in \mathbb{R}^m$ as follows:

$$A\,\mathbf{F}_{\text{mus}} = B\,\mathbf{F}_{\text{ext}}, \tag{19}$$

where A is a $p \times m$ matrix and B is a $p \times 3$ matrix, where the number of rows p equals the minimal number of scalar static equilibrium equations, generally equal to the number of degrees of freedom. In a static configuration, the muscle force directions are specified, so we only solve for the muscle force magnitudes $\mathbf{F}_{\text{mus}}$. The matrices A and B contain geometrical parameters such as instantaneous muscle moment arms and external force moment arms at the current limb configuration. Equation 19 assumes that the external force to be produced is much larger than limb weight. For instance, for the two-segment limb of Figure S7, $p = 2$ with the equations obtainable by moment balance of the whole limb OAB about O and the segment AB about A. We minimize the following muscle-force-based power law metabolic cost:

$$\dot{E}_{\text{task}} = c_1 F_{\text{mus},1}^{\gamma} + c_2 F_{\text{mus},2}^{\gamma} + \ldots + c_m F_{\text{mus,m}}^{\gamma} = C^T \mathbf{F}_{\text{mus}}^{\gamma}, \tag{20}$$

where the matrix $C = [c_1;\ c_2;\ \ldots\ c_m]$ and $\mathbf{F}_{\text{mus}}^{\gamma}$ is defined as $[F_1^{\gamma};\ F_2^{\gamma};\ \ldots]$. To solve the constrained optimization problem, we define the Lagrangian L as:

$$L = C^T \mathbf{F}_{\text{mus}}^{\gamma} + \xi^T (A\,\mathbf{F}_{\text{mus}} - B\,\mathbf{F}_{\text{ext}})$$

where ξ contains the Lagrange multipliers $[\xi_1;\ \xi_2;\ \ldots\ \xi_p]$. Differentiating this Lagrangian, that is, computing the gradient ∇L with respect to the unknown muscle force magnitudes $\mathbf{F}_{\text{mus}}$, and setting this derivative equal to zero gives:

$$\nabla L = \gamma C^T \mathbf{F}_{\text{mus}}^{\gamma-1} + A^T \xi = 0. \tag{21}$$

Equations 19 and 30 together provide $p+m$ linear equations in the $p+m$ unknowns in the ξ and $\mathbf{F}_{\text{mus}}$.

These equations 19 and 30 have solutions with an elegant structure that implies a simple scaling strategy for producing different external force levels. To show this, assume that one needs to produce scaled versions of a fixed external force. That is, $\mathbf{F}_{\text{ext}} = \mu\mathbf{F}_0$, where $\mathbf{F}_0 \in \mathbb{R}^3$ is a fixed force and $\mu \in \mathbb{R}$ scales this force linearly to produce the external force $\mathbf{F}_{\text{ext}}$. We can rewrite the static equilibrium (equation 19) as:

$$A\,\mathbf{F}_{\text{mus}} = \mu B \mathbf{F}_0. \tag{22}$$

We now posit and show that the solution is of the form:

$$\mathbf{F}_{\text{mus}} = \mu \mathbf{F}_{\text{mus0}} \ \text{ and } \xi = \mu^{\gamma-1}\xi_0, \tag{23}$$

where $\mathbf{F}_{\text{mus}}$ is a fixed set of muscle force magnitudes. To verify the correctness of this solution, we substitute the solution form into equations 19 and 30, which gives the following two equations that are independent of μ:

$$\mu A \mathbf{F}_{\text{mus0}} = \mu B \mathbf{F}_0 \text{ and } \gamma C^T \mathbf{F}_{\text{mus0}}^{\gamma-1} + A^T \xi_0 = 0 \tag{24}$$

These equations allow us to solve for $\mathbf{F}_{\text{mus0}}$ and ξ_0 without any dependence on μ, so how the muscle force magnitudes depend on μ is captured by equation 23. Thus, we predict that linearly scaling the external force is energy-optimally accomplished by linearly scaling the muscle force magnitudes. Such linear scaling is observed in producing finger forces and arm forces[8,9].

Corollary 1: Whole limb cost scales the same way as muscle-level costs for static tasks. Substituting the muscle force solution (equation 23) into the metabolic cost expression (equation 27) shows that the total metabolic cost will scale like μ^{γ}:

$$\text{Metabolic cost } = C^T \mathbf{F}_{\text{mus}}^{\gamma} = \mu^{\gamma} (C^T \mathbf{F}_{\text{mus0}}^{\gamma}) \tag{25}$$

Thus, given that the external force magnitude is $|\mathbf{F}_{\text{ext}}| = \mu |\mathbf{F}_0|$ is proportional to μ, the metabolic cost scales like external force raised to the power γ, when the external force is simply scaled. This provides self-consistency of our power-law metabolic approach across scales and ensures that the model initially used to obtain the metabolic cost model in terms of external force has no loss of generality.

Corollary 2: Optimality of linear muscle force and torque scaling strategy. At a given configuration, the joint torques are linear functions of muscle forces, given by:

$$\tau = D\mathbf{F}_{\text{mus}} = \mu\, D\mathbf{F}_{\text{mus0}}, \tag{26}$$

where D is a matrix of muscle moment arms. Thus, each of the joint torques is proportional to μ and scales linearly with the external force magnitude. So, when scaling the external force in a fixed limb configuration, the metabolic cost also scales like joint torque magnitude to the power γ. Recall that the theorem and the corollaries rely on fixing the configuration and having the external force be much higher than gravity, so gravity terms may be ignored. When gravity terms are substantial, the simple solution structure described above does not hold.

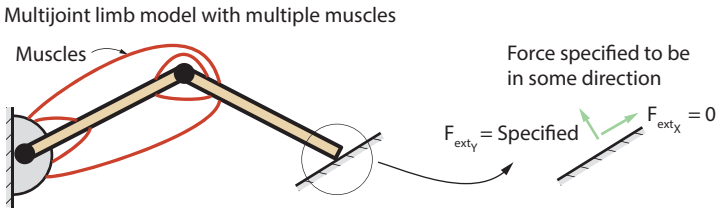

Figure S7. A multi-segment multi-joint limb with multiple muscles, applying an external force along some fixed direction.

S4.2 Dynamic condition with force-rate costs

The multi-joint limb has m muscles (figure S7A) and p degrees of freedom. The limb is at rest and the task is to apply a 3D external force $\mathbf{F}_{\text{ext}}$ of different magnitudes along a fixed direction: the external force $\mathbf{F}_{\text{ext}}$ can be considered a scaled version $\mu\mathbf{F}_0$ of some nominal 3D external force $\mathbf{F}_0 \in \mathbb{R}^3$, which decides the desired direction. Then, force rate is given by $\dot{\mathbf{F}}_{\text{ext}} = \dot{\mu}\mathbf{F}_0$ where $\dot{\mu}$ is changes the force rate along the fixed direction. Because the force rate is always in the direction of the force, the force remains along a fixed direction for all time. The muscle force magnitudes are $\mathbf{F}_{\text{mus}} = [F_1;\, F_2;\, \ldots] \in \mathbb{R}^m$ and we minimize the metabolic cost with a power law relation on muscle force and force rate magnitudes:

$$\begin{aligned} \dot{E}_{\text{task}} &= c_1 F_{\text{mus},1}^{\gamma_1} + c_2 F_{\text{mus},2}^{\gamma_1} + \ldots + c_m F_{\text{mus,m}}^{\gamma_1} + d_1 \dot{F}_{\text{mus},1}^{\gamma_2} + d_2 \dot{F}_{\text{mus},2}^{\gamma_2} + \ldots + d_m \dot{F}_{\text{mus,m}}^{\gamma_2} \\ &= C^T \mathbf{F}_{\text{mus}}^{\gamma_1} + D^T \dot{\mathbf{F}}_{\text{mus}}^{\gamma_2}, \end{aligned} \tag{27}$$

where the matrix $C = [c_1;\, c_2;\, \ldots\, c_m]$, $D = [d_1;\, d_2;\, \ldots\, d_m]$, $\mathbf{F}_{\text{mus}}^{\gamma_1} = [F_1^{\gamma_1};\, F_2^{\gamma_1};\, \ldots]$ and $\dot{\mathbf{F}}_{\text{mus}}^{\gamma_2} = [\dot{F}_1^{\gamma_2};\, \dot{F}_2^{\gamma_2};\, \ldots]$.

What is proved. We show that if the optimal muscle force for the nominal external force and force rate ($\mu = 1$ and $\dot{\mu} = 1$) is $\mathbf{F}_{\text{mus0}}$, the optimal muscle force for any other external force is given by $\mathbf{F}_{\text{mus}} = \mu\mathbf{F}_{\text{mus0}}$ and the optimal force rate is $\dot{\mathbf{F}}_{\text{mus}} = \dot{\mu}\mathbf{F}_{\text{mus0}}$.

Proof. In terms of notation and proof technique, we closely follow our earlier work in the previous section, which proves a special case of zero force rates. The condition that the whole limb is in static equilibrium can be written as a linear equation in the list of m muscle force magnitudes $\mathbf{F}_{\text{mus}} \in \mathbb{R}^m$ as follows:

$$A\,\mathbf{F}_{\text{mus}} = B\,\mathbf{F}_{\text{ext}} = \mu B\mathbf{F}_0, \tag{28}$$

where A is a $p \times m$ matrix and B is a $p \times 3$ matrix containing geometric parameters, where the number of rows p generally equals the number of degrees of freedom. Equations 28-29 ignores gravity, as noted earlier. Taking the derivative of equation 28 gives the condition for force rates:

$$A\,\dot{\mathbf{F}}_{\text{mus}} = B\,\dot{\mathbf{F}}_{\text{ext}} = \dot{\mu} B\mathbf{F}_0 \tag{29}$$

These equations serve as equality constraints for the optimization.

The Lagrangian L for the constrained optimization problem is:

$$L = C^T \mathbf{F}_{\text{mus}}^{\gamma_1} + D^T \dot{\mathbf{F}}_{\text{mus}}^{\gamma_2} + \xi^T (A\,\mathbf{F}_{\text{mus}} - B\,\mathbf{F}_{\text{ext}}) + \lambda^T (A\,\dot{\mathbf{F}}_{\text{mus}} - B\,\dot{\mathbf{F}}_{\text{ext}}),$$

where ξ contains the Lagrange multipliers $[\xi_1;\ \xi_2;\ \ldots\ \xi_p]$ and λ contains the Lagrange multipliers $[\lambda_1;\ \lambda_2;\ \ldots\ \lambda_p]$. Computing the gradients $\nabla_F L$ and $\nabla_{\dot{F}} L$ with respect to the unknown muscle force $\mathbf{F}_{\text{mus}}$ and force rate magnitudes $\dot{\mathbf{F}}_{\text{mus}}$, and setting these gradients equal to zero gives:

$$\begin{aligned} \nabla L &= \gamma_1 C^T \mathbf{F}_{\text{mus}}^{\gamma_1 - 1} + A^T \xi = 0 \text{ and} && (30) \\ \nabla L &= \gamma_2 D^T \dot{\mathbf{F}}_{\text{mus}}^{\gamma_2 - 1} + A^T \lambda = 0. && (31) \end{aligned}$$

Equations 28 and 29 together provide $2p+2m$ linear equations in the $2p+2m$ unknowns in the ξ , $\mathbf{F}_{\text{mus}}$, λ , $\dot{\mathbf{F}}_{\text{mus}}$.

We now show that these equations 28, 29, 30, and 31 imply the linear scaling strategy. That is, we show that the solution is of the form:

$$\begin{aligned} \mathbf{F}_{\text{mus}} &= \mu \mathbf{F}_{\text{mus0}} \text{ and } \xi = \mu^{\gamma_1 - 1} \xi_0, \text{ and} && (32) \\ \dot{\mathbf{F}}_{\text{mus}} &= \dot{\mu} \mathbf{F}_{\text{mus0}} \text{ and } \lambda = \dot{\mu}^{\gamma_2 - 1} \lambda_0, && (33) \end{aligned}$$

where $\mathbf{F}_{\text{mus0}}$ and $\dot{\mathbf{F}}_{\text{mus0}}$ are a fixed set of muscle force and force rate magnitudes respectively. To show this, we substitute this proposed solution form into equations 28, 29, 30, and 31, which gives the following three equations:

$$\mu A \mathbf{F}_{\text{mus0}} = \mu B \mathbf{F}_0, \text{ and } \gamma C^T \mathbf{F}_{\text{mus0}}^{\gamma_1 - 1} + A^T \xi_0 = 0, \text{ and } \gamma D^T \mathbf{F}_{\text{mus0}}^{\gamma_2 - 1} + A^T \lambda_0 = 0 \quad (34)$$

These equations (equation 34) have no dependence on μ and $\dot{\mu}$, and thus can be solved for $\mathbf{F}_{\text{mus0}}$, ξ_0 and λ_0 without any dependence on μ and $\dot{\mu}$. This non-dependency of $\mathbf{F}_{\text{mus0}}$ on μ and $\dot{\mu}$ is consistent with the assumed solution form (equations 32 and 33). Thus, the proposed solution does correctly specify how the muscle force magnitudes and the force rate magnitudes depend on μ and $\dot{\mu}$ respectively, thereby establishing the linear scaling strategy.

Corollary 1: Muscle-level power law cost implies whole limb-level power law costs. Substituting the solution for muscle force and force rates (equation 32-33) into the whole limb or 'whole body' metabolic cost expression (equation 27) gives:

$$\begin{aligned} \text{Whole limb metabolic cost} &= C^T \mathbf{F}_{\text{mus}}^{\gamma_1} + D^T \dot{\mathbf{F}}_{\text{mus}}^{\gamma_2} \\ &= C^T (\mu \mathbf{F}_{\text{mus0}})^{\gamma_1} + D^T (\dot{\mu} \mathbf{F}_{\text{mus0}})^{\gamma_2} \\ &= \mu^{\gamma_1} \cdot C^T \mathbf{F}_{\text{mus0}}^{\gamma_1} + \dot{\mu}^{\gamma_2} \cdot D^T \mathbf{F}_{\text{mus0}}^{\gamma_2}. \end{aligned}$$

Given that μ and $\dot{\mu}$ are respectively proportional to the external force and force rates, we have shown that the whole limb metabolic cost also scales in the same power law manner (same exponents) with respect to the external force and force rate as do the muscles with respect to the muscle forces and force rates.

Corollary 2: Linear scaling strategy is optimal for joint torques. At a given configuration, the joint torques are linear functions of muscle forces, given by:

$$\tau = D \mathbf{F}_{\text{mus}} = \mu\, D \mathbf{F}_{\text{mus0}} = \mu\, \tau_0, \quad (35)$$

where D is a matrix of muscle moment arms and τ_0 is the nominal joint torques when $\mu = 1$. Equation 35 shows that the linear scaling strategy is also true for joint torques: joint torques for some external force are scaled versions of the joint torques for a particular external force in the same direction. Differentiating equation 35, we obtain the analogous linear scaling strategy for the joint torque rates:

$$\dot{\tau} = D \dot{\mathbf{F}}_{\text{mus}} = \dot{\mu}\, D \mathbf{F}_{\text{mus0}} = \dot{\mu}\, \tau_0. \quad (36)$$

Other remarks. While we have shown the three results for metabolic costs that are functions of force and force rate, they are true for when the metabolic cost depends in similar power law fashion on higher derivatives of force as well.

The theorem and corollaries, as proved, rely on ignoring gravity. However, it can be shown that the theorem and corollaries are also true in the presence of gravity in the following special case: the multi-segment system is such that it can be at rest with muscles turned off while in contact with the external surface. The 2D two segment system shown in figure S7 has this property. While such a system is in rest with such passive turned-off muscles, there is no metabolic cost, but there is an external force applied on the surface, $\mathbf{F}_{\text{passive}}$. In this situation, all the results are true when we replace $\mathbf{F}_{\text{ext}} - \mathbf{F}_{\text{passive}}$.

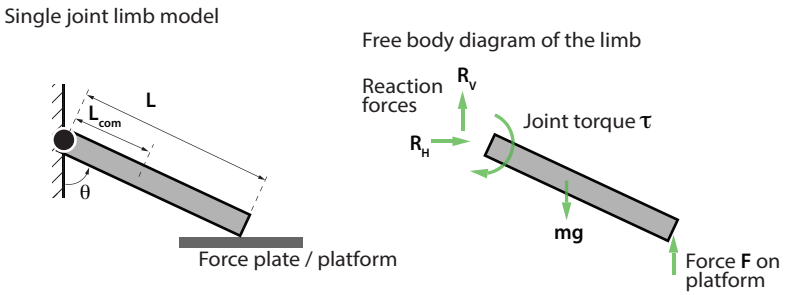

Figure S8. Single joint model of a limb used for bilateral force sharing.

Parameters	**Value**	**Parameters** (N/mm)	**Value**
MFR	8 impulses/s	n	5
PFR1	45 impulses/s	K_S	0.9 mM
PFRD	10 impulses/sec	$V_{\max}$	50 mM/s
g_e	1	k_b	20
a	0.0283	k_u	1
b	0.0384	B_{total}	200 mM
c	4.19	A	1 mM
cv_{ISI}	0.2	$C_{f,\max}$	3 mM
α	0.1	m	4
K_F	0.75 mM	b_F	35
τ_F	0.75 s^{-1}	T_L	0.09 s^{-1}
N_{MU}	120		

Table S2. Parameters for model of muscle energetics including recruitment, rate coding, calcium, and force dynamics. While the specific values for most parameters do not matter for the nonlinearity to emerge, one contributing condition for a convex nonlinearity is $n > m$.

References

1. Fuglevand, A. J., Winter, D. A. & Patla, A. E. Models of recruitment and rate coding organization in motor-unit pools. *J. neurophysiology* **70**, 2470–2488 (1993).
2. Gerritsen, K. G., van den Bogert, A. J., Hulliger, M. & Zernicke, R. F. Intrinsic muscle properties facilitate locomotor control—a computer simulation study. *Mot. control* **2**, 206–220 (1998).
3. Ackermann, M. & Van den Bogert, A. J. Optimality principles for model-based prediction of human gait. *J. biomechanics* **43**, 1055–1060 (2010).
4. Handford, M. L. & Srinivasan, M. Robotic lower limb prosthesis design through simultaneous computer optimizations of human and prosthesis costs. *Sci. reports* **6**, 19983 (2016).
5. Umberger, B. R., Gerritsen, K. G. & Martin, P. E. A model of human muscle energy expenditure. *Comput. methods biomechanics biomedical engineering* **6**, 99–111 (2003).
6. Bhargava, L. J., Pandy, M. G. & Anderson, F. C. A phenomenological model for estimating metabolic energy consumption in muscle contraction. *J. biomechanics* **37**, 81–88 (2004).
7. van der Zee, T. J. & Kuo, A. D. The high energetic cost of rapid force development in muscle. *J. Exp. Biol.* **224**, jeb233965 (2021).
8. Valero-Cuevas, F. J. Predictive modulation of muscle coordination pattern magnitude scales fingertip force magnitude over the voluntary range. *J. Neurophysiol.* **83**, 1469–1479 (2000).
9. Morrison, S. & Newell, K. Interlimb coordination as a function of isometric force output. *J. Mot. Behav.* **30**, 323–342 (1998).